

SPE FAR: Shear Wave Generation

Presented to:

SPE FAR Independent Assessment Review

TEAM:

SNL: Andréa Darrh, Miles Bodmer, **Christian Poppeliers** (presenter)

LANL: Ting Chen, Carene Larmat, Scott Phillips

LLNL: Arben Pitarka

2 November, 2021



BLUF: observe/quantify shear wave generation from a buried explosion

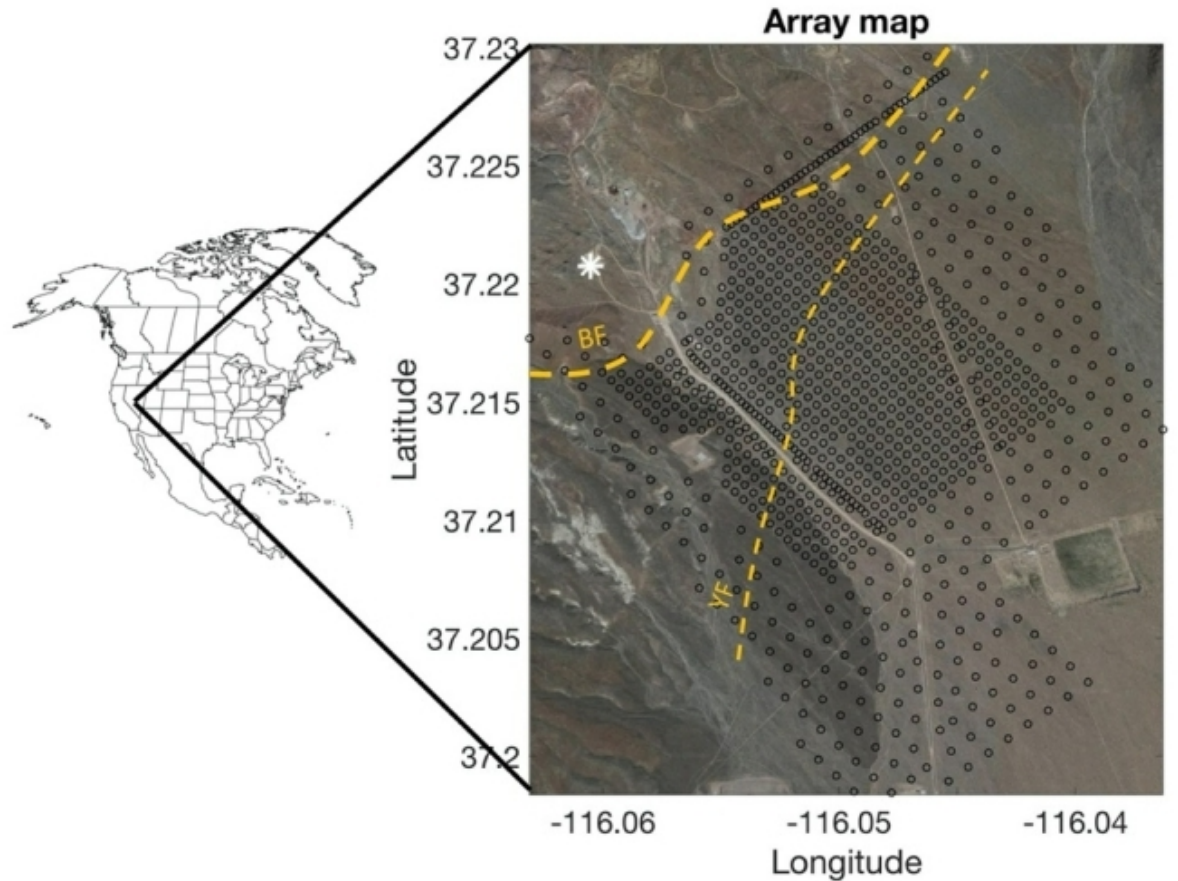


1. Analysis shows that shear waves generated from both geologic structure (SPE-I) stochastic heterogeneities (SPE-I and SPE-II)
 - azimuthally dependent!
 - high-frequency shear generation saturates at about 1km propagation distance
2. Summary of Analysis
 - Sandia National Labs
 - Large N arrays to observed/quantify shear waves from scattering
 - “bulk” wavefield
 - simulations of explosion-generated wavefield: scattering from stochastic heterogeneities
 - Lawrence Livermore National Labs
 - Large N arrays to observe/quantify shear waves from scattering
 - discrete wave arrivals
 - simulations: scattering from geologic structure and stochastic heterogeneity
 - Los Alamos National Labs
 - simulations of explosion-generated wavefields
 - scattering from geologic structure

SPE Phase I



- SPE Phase I: Large N array
 - Single event (“SPE 5”)
 - WP in granite
 - Most of the Large N was on the adjacent alluvium
 - Boundary Fault (BF):
 - Approximately vertical boundary between granite and alluvium
 - Expect significant wavefield modification
 - Likely near-source P-to-S conversions
- Goal: observe near-source wavefield modification from significant structure
 - We analyzed vertical-component geophone data for coherence and wave propagation



SPE Phase I: Large N analysis strategy

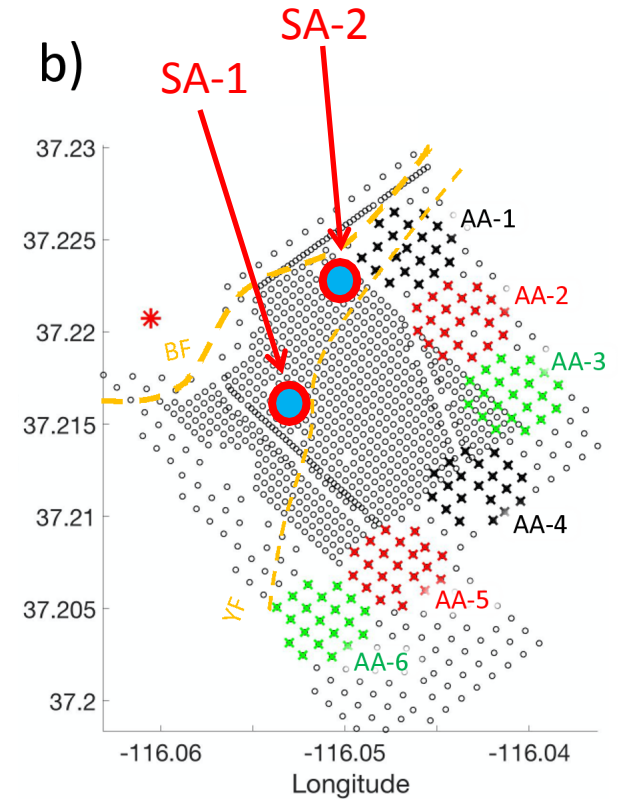
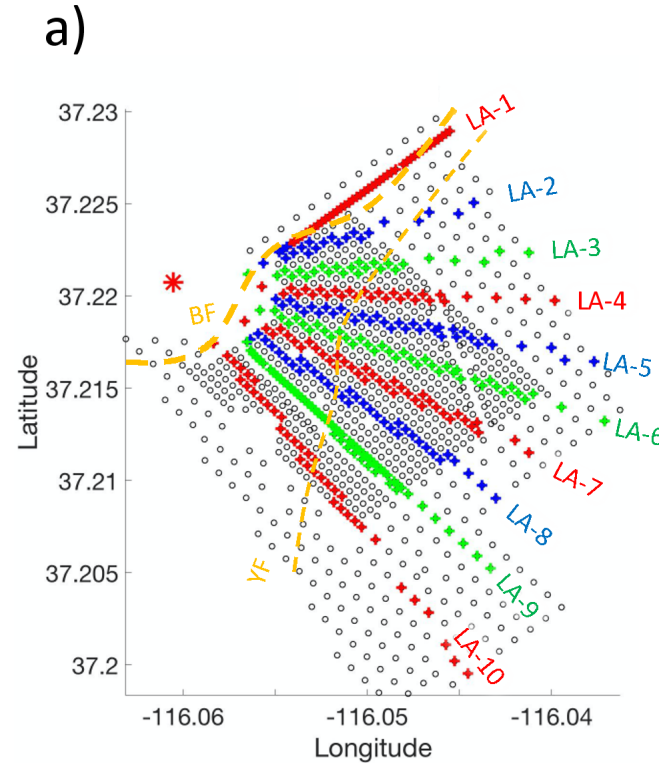
- Method: subset Large-N into “sub arrays”
- Question: How does BF diminish the “isotropic-ness” of the original explosion-generated wavefield?

a) Linear arrays

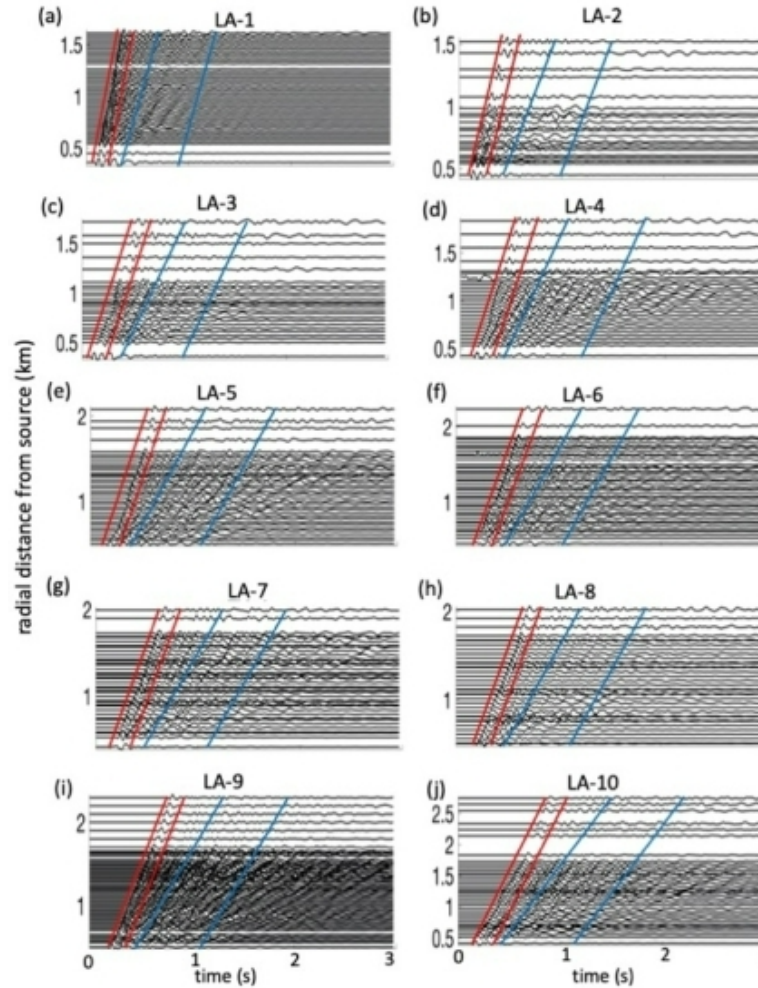
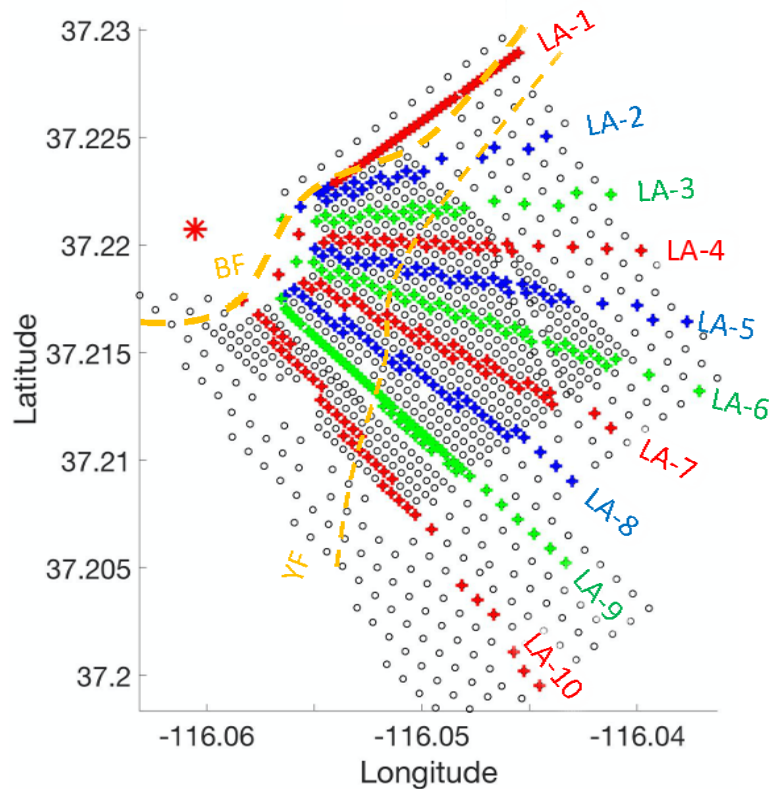
- a) Goal: wavefield coherence as a function of position

b) Areal arrays

- a) Goal: wavefield propagation vector as a function of proximity to BF

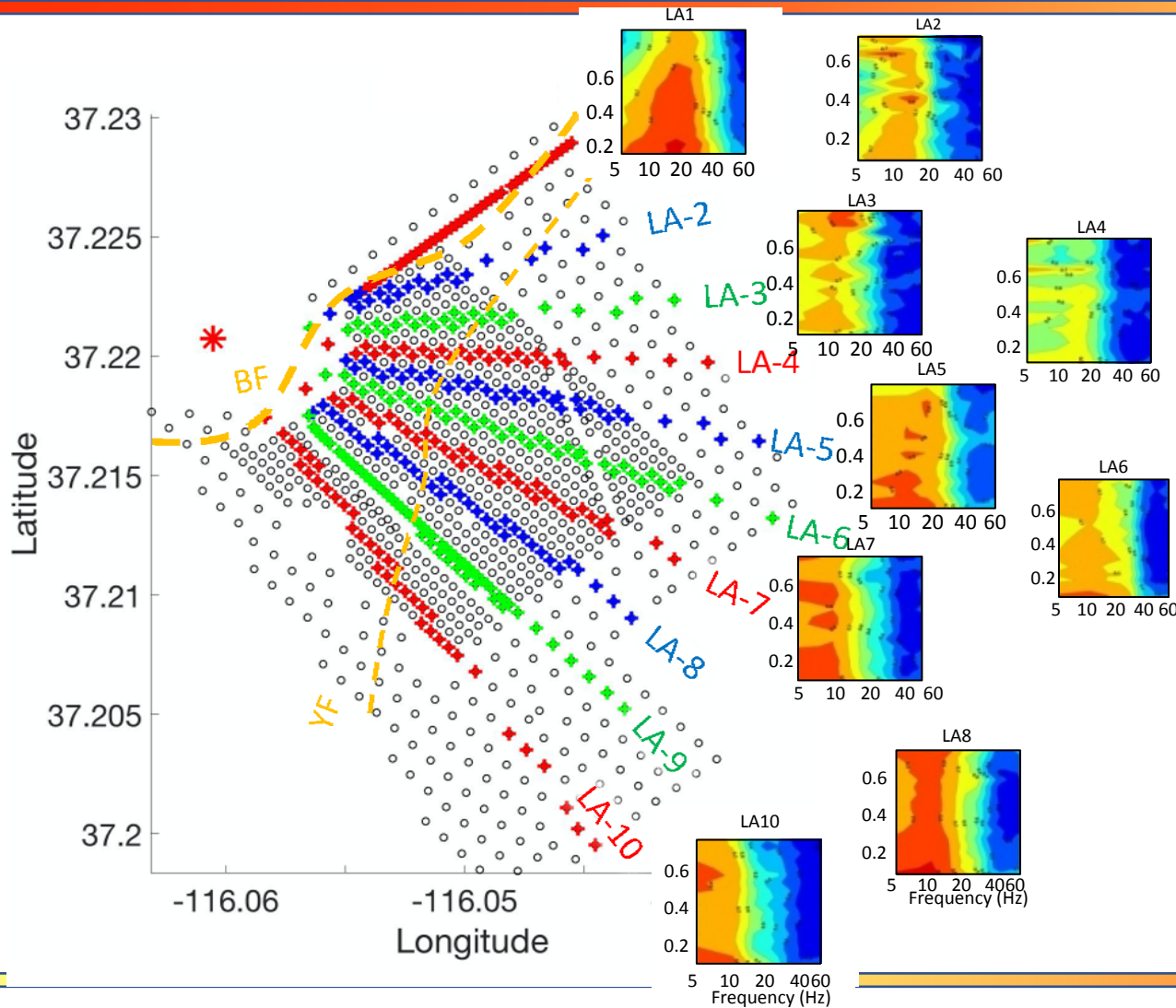


SPE Phase I: Large N raw data

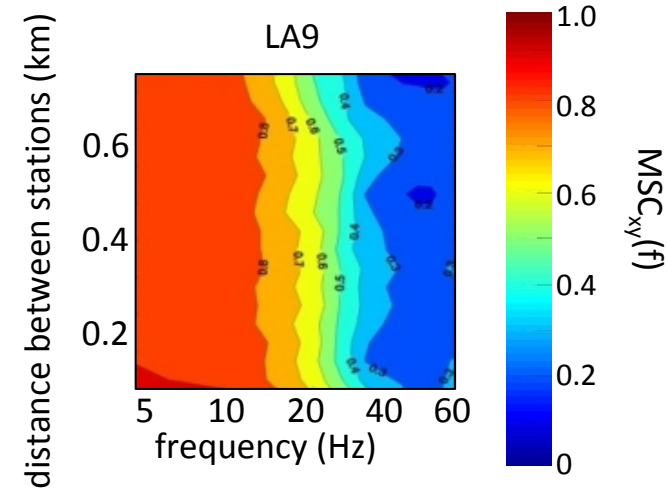


Note the increased amplitude of surface waves as the angular distance from the BF increases

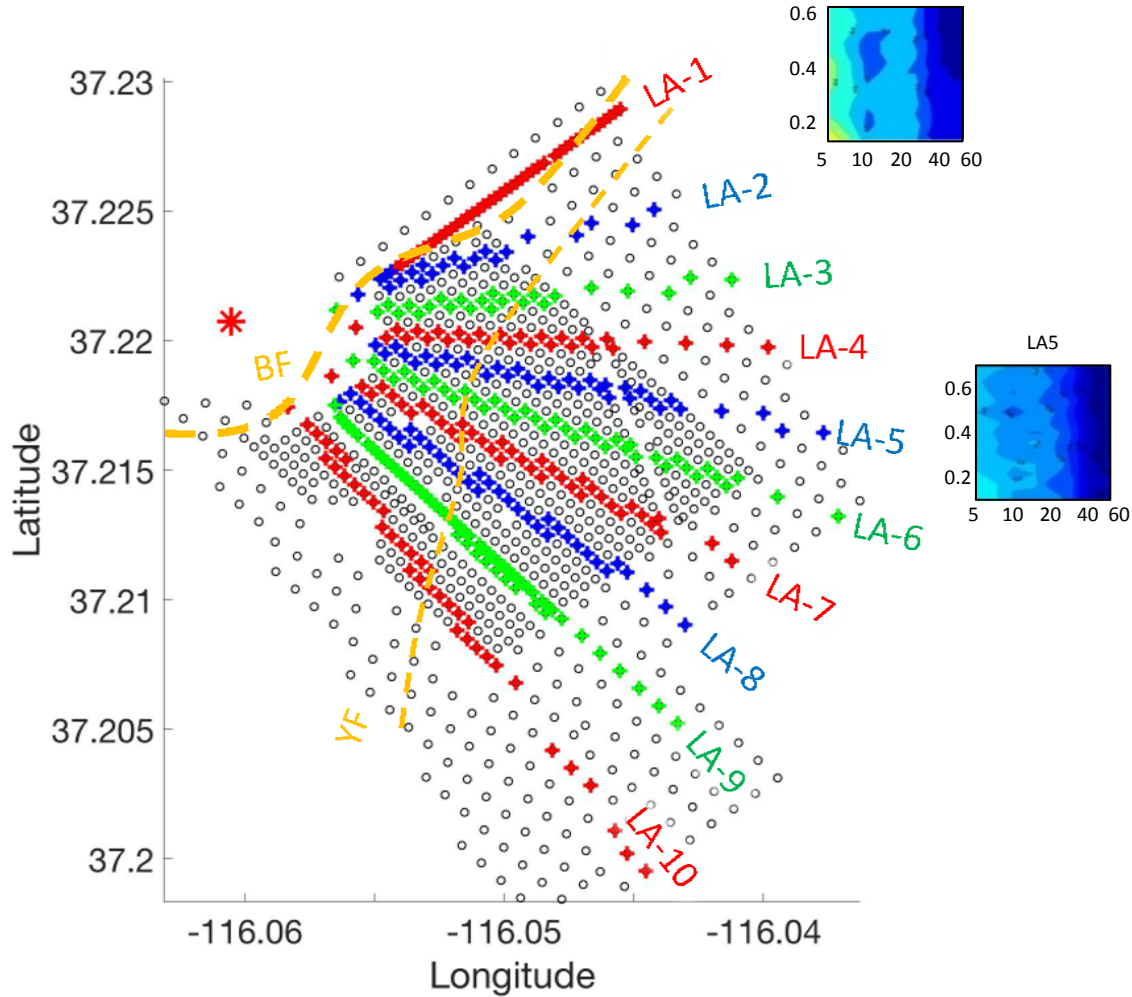
SPE - I: wavefield coherency: direct P



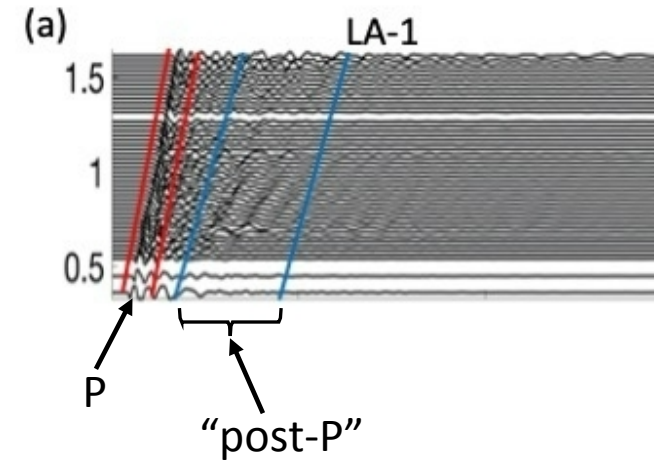
- Highest wavefield coherency for fault-parallel and fault-perpendicular wave propagation
- Generally, higher coherency for lower frequencies
- Interpretation: fault is preferentially scattering the direct P: “anisotropic scattering”



SPE - I: wavefield coherency: post-P



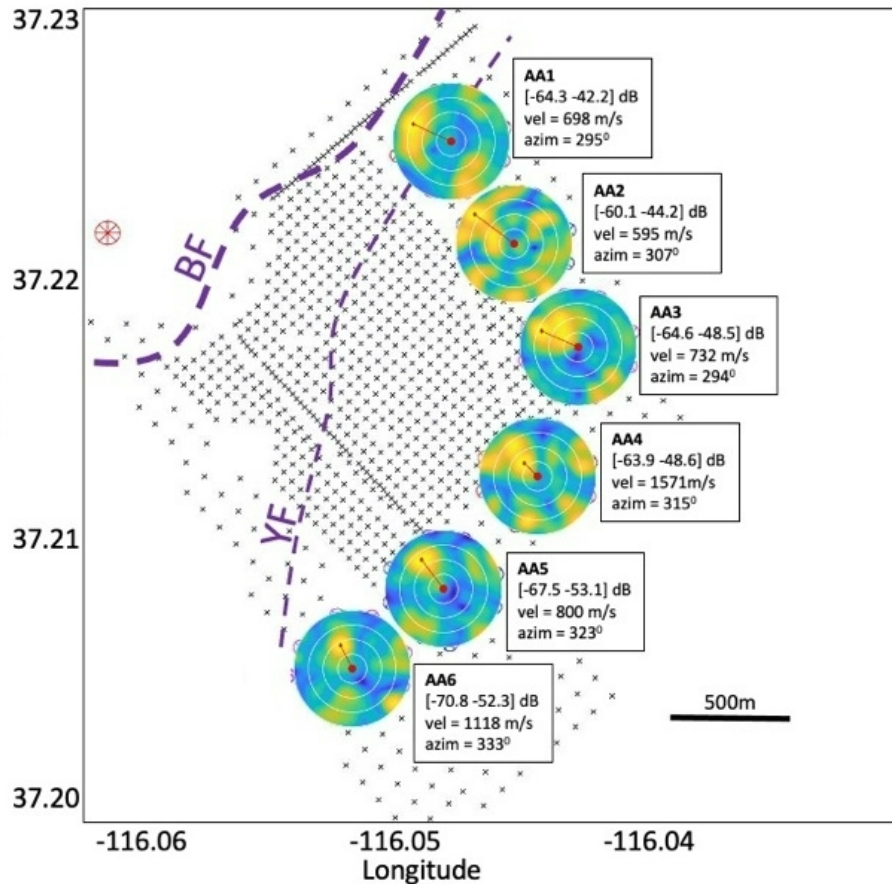
- Highest wavefield coherency for fault-parallel
- For all other propagation directions, the post-P wavefield is virtually incoherent for all frequencies.
- Interpretation: fault is preferentially scattering the post-P: “anisotropic scattering”



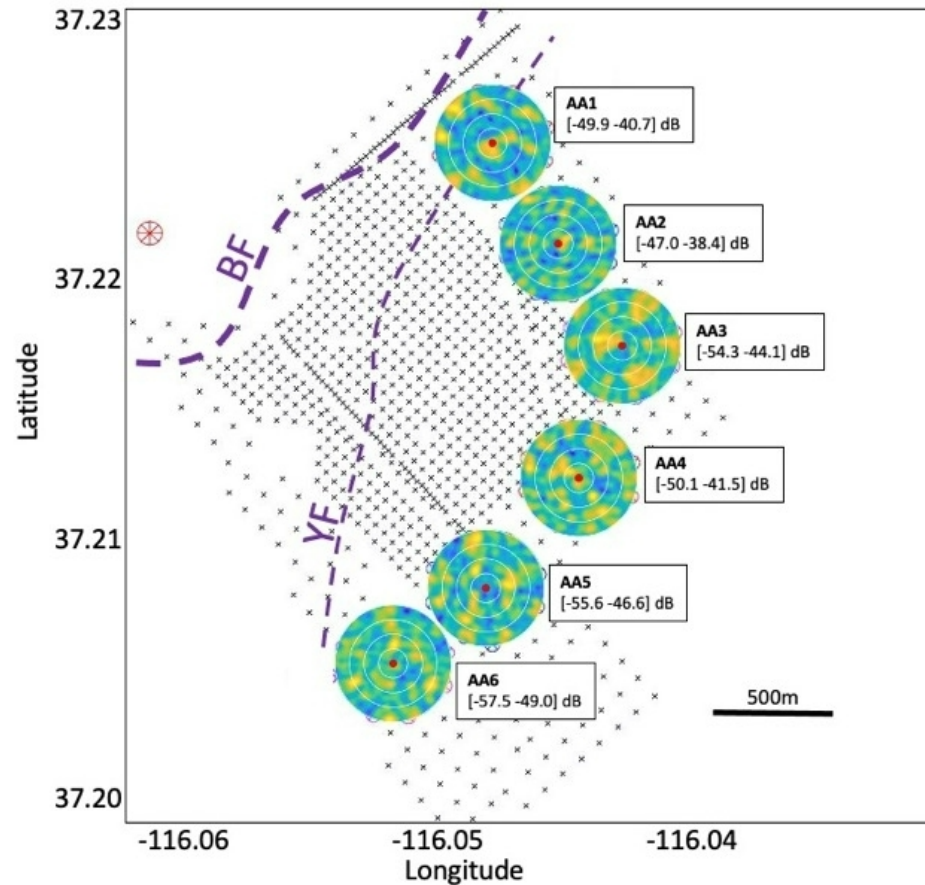
SPE - I: wavefield propagation (2-6 Hz)



Direct P



Post P

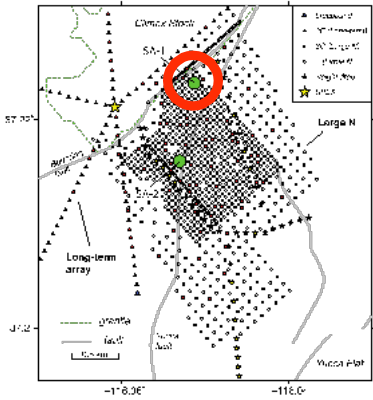


Array Processing for areal arrays

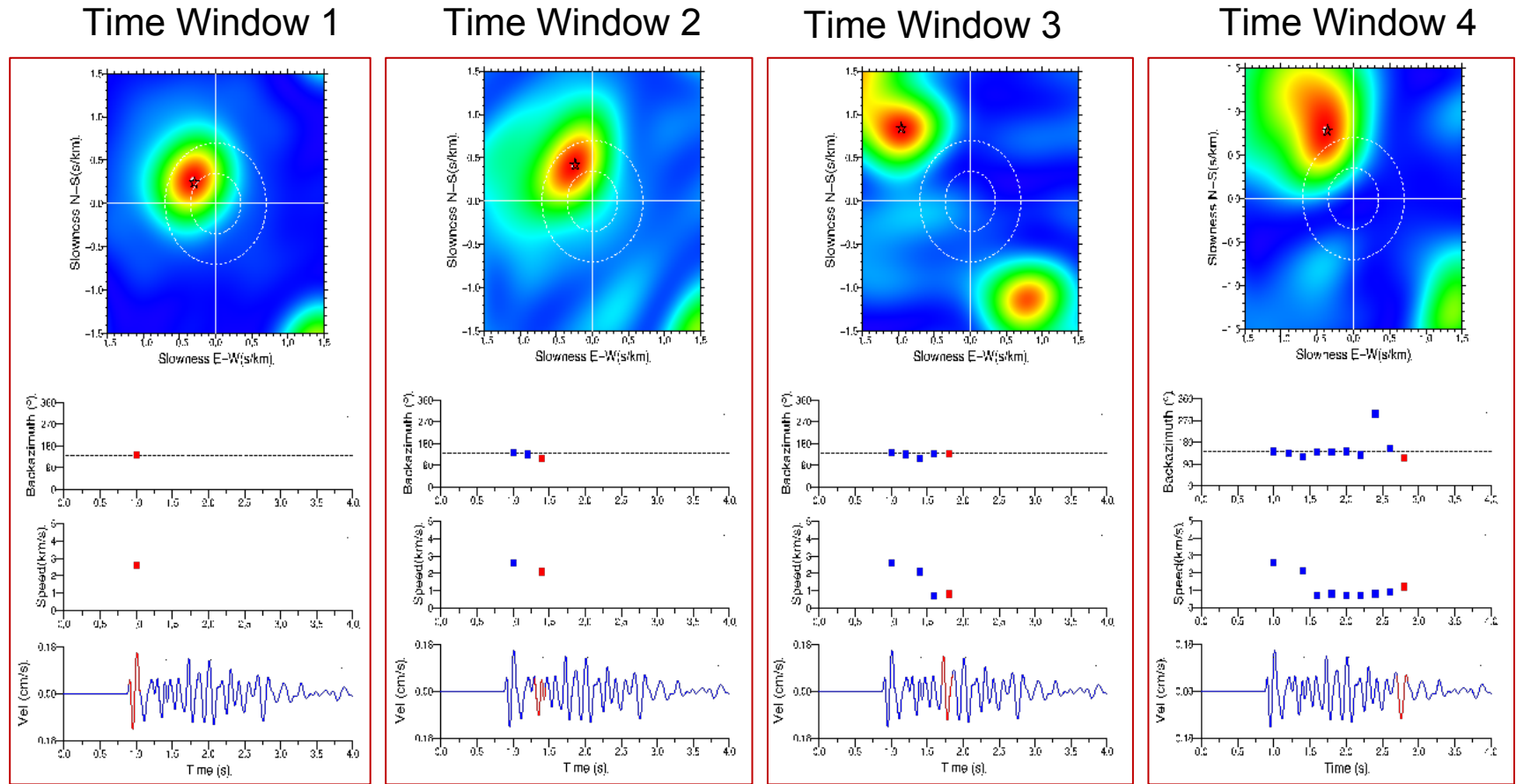
- Direct P: Substantial amount of low-frequency scattered P waves radiating normal to fault
- Post-P: scattered energy appears to have no directional preference

Darrh, A., Poppeliers, C., Preston, L., 2019. Azimuthally Dependent Seismic Wave Coherence at the Source Physics Experiment Large-N Array., *Bull. Seis. Soc. Am.*, **109**(5): 1935-1947.

SPE - I: wavefield propagation (3-8 Hz)

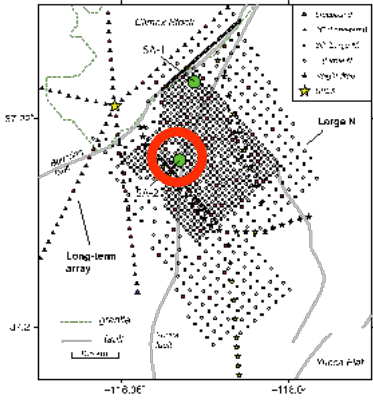


- P-wave radiating normal to BF
- scattered wave packets also appear to radiate normal to BF
- Interpretation: scattering from the BF is a strong source of shear waves

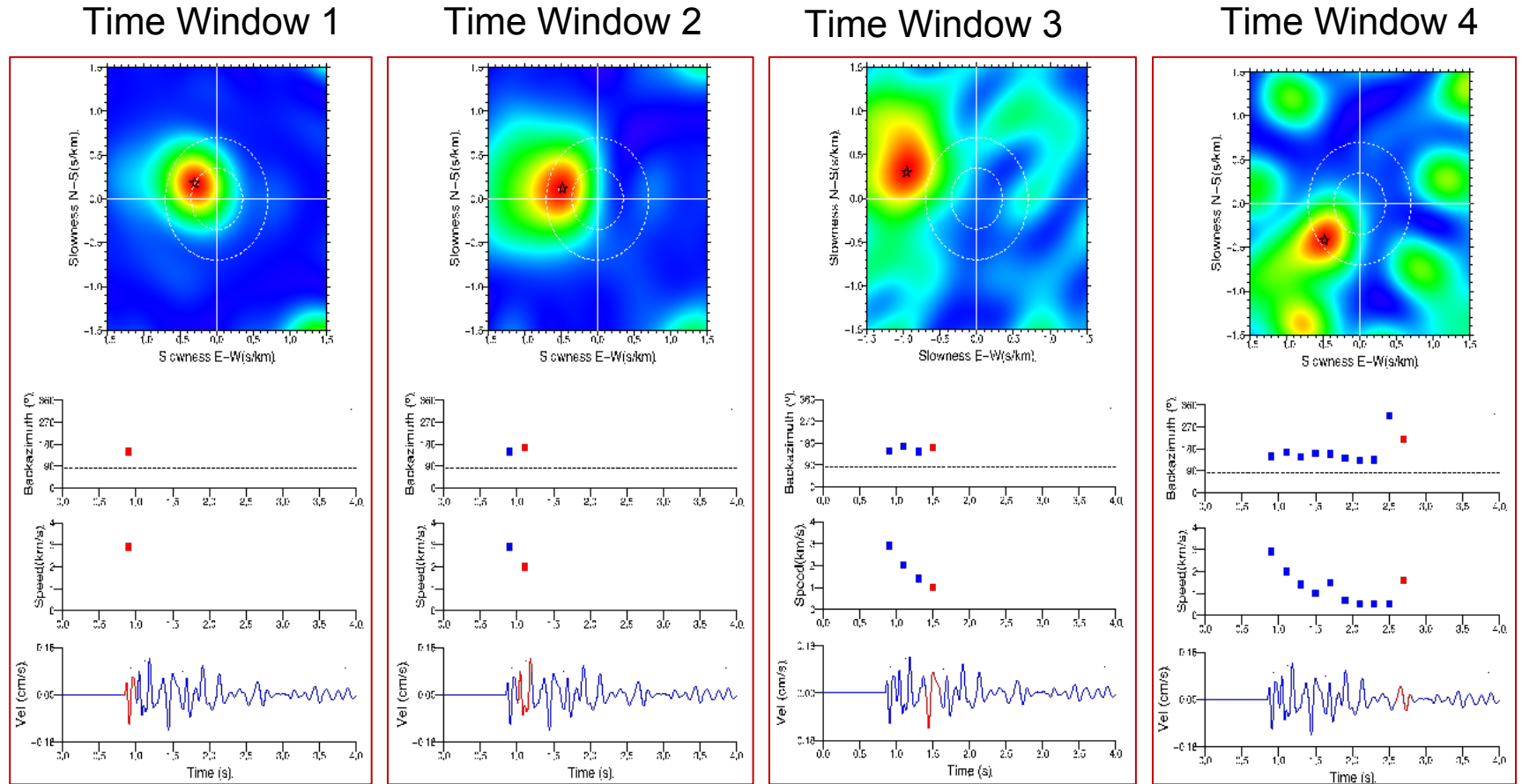


figures from Arben Pitarka, Lawrence Livermore National Lab.

SPE - I: wavefield propagation (3-8 Hz)

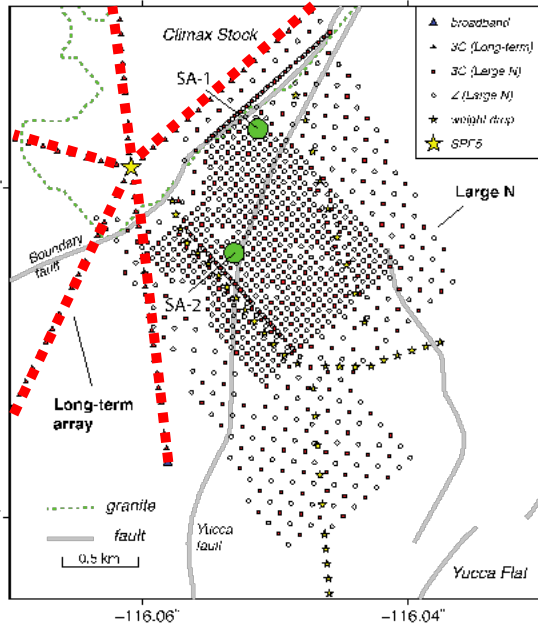


- All waves radiating from the source

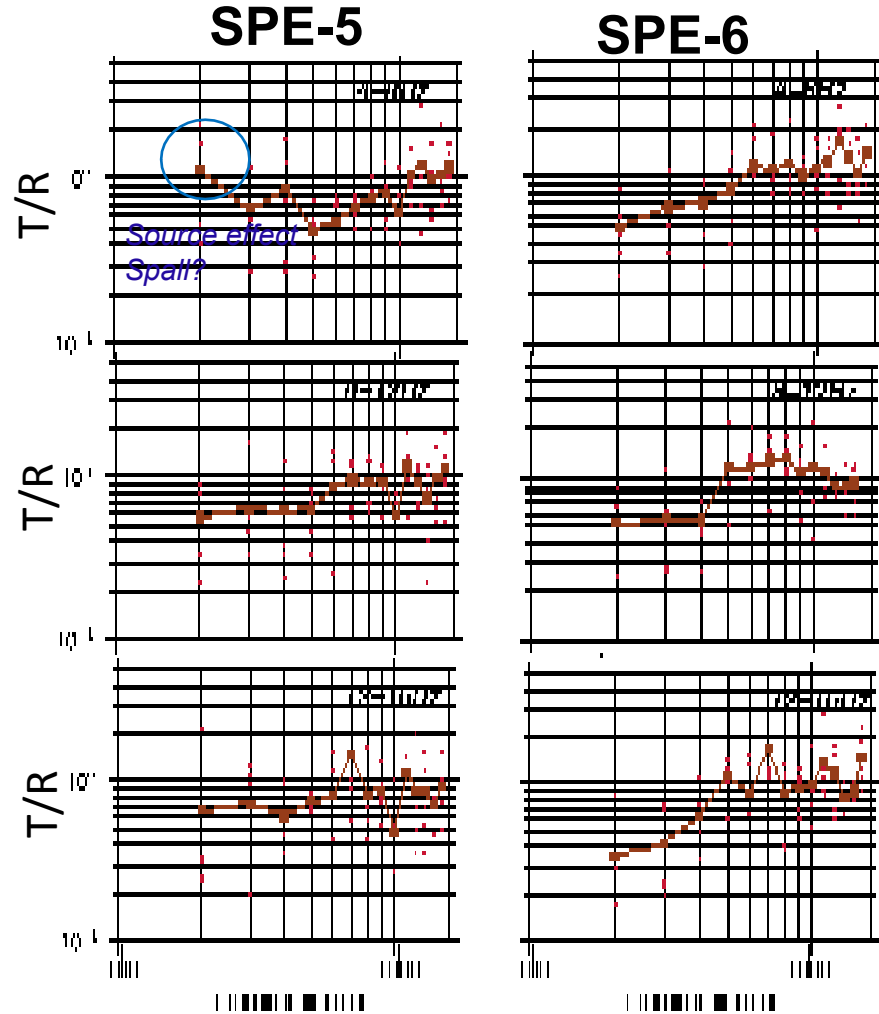


Pitarka, A., R. Mellors (2021). Using Dense Array Waveform Correlations to Build a Velocity Model with Stochastic Variability, Bull. Seis. Soc. Am, XX, 1-21

SPE - I: Other linear arrays



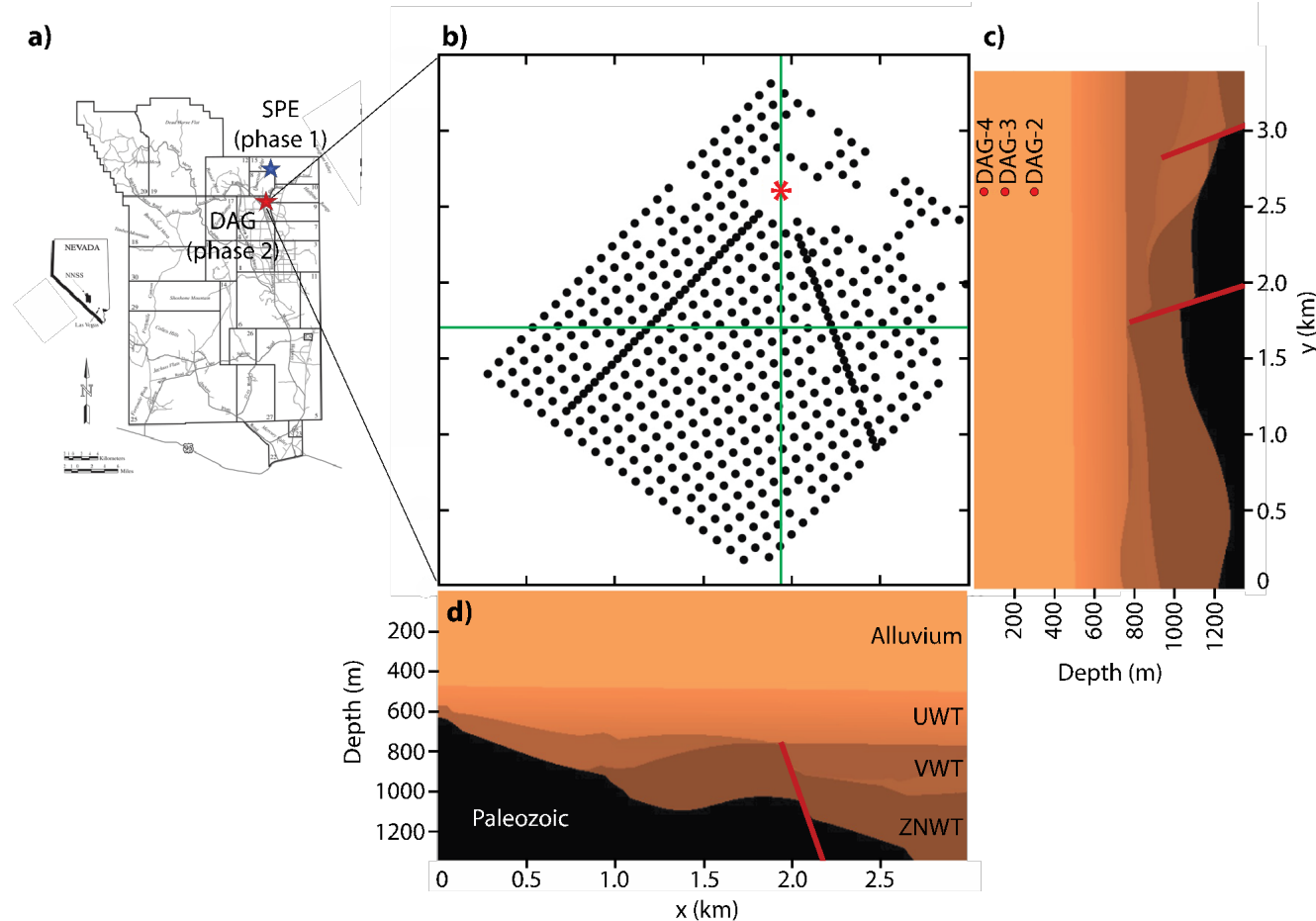
figures from Arben Pitarka,
Lawrence Livermore
National Lab.



- ratio of transverse-to-radial (T/R) component seismic energy
- T/R is low for small distance, increases as distance increases
- T/R generally stabilizes at a distance of ~600m, suggesting that the wavefield becomes diffusive.
- Suggests that transverse component energy is a result of $P \rightarrow S$ scattering

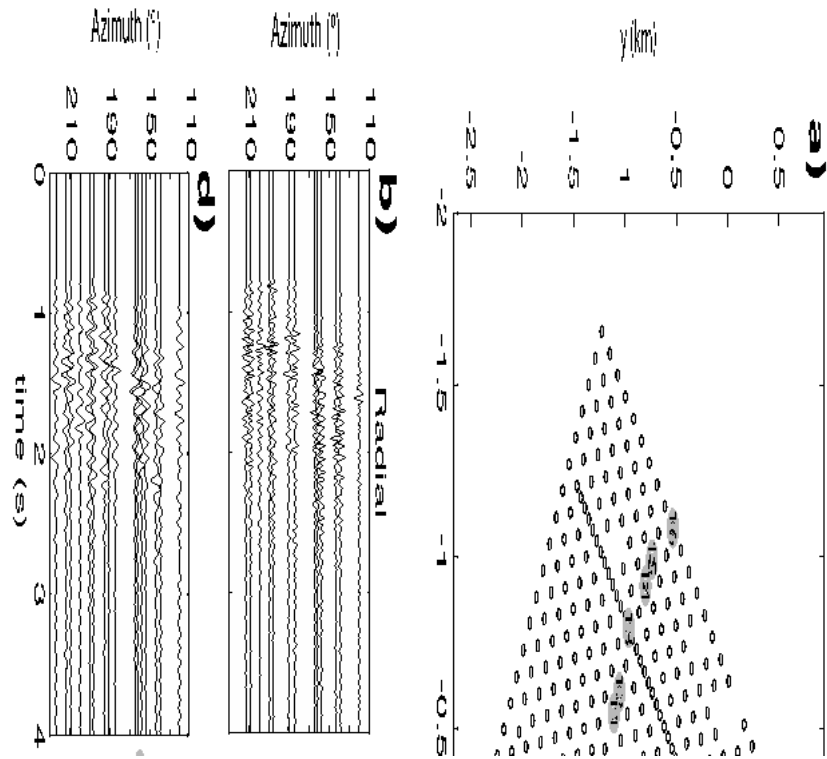
SPE Phase II (Dry Alluvium Geology)

- SPE Phase II (DAG): Large N array
 - Three events DAG 2-4
 - WP in dry alluvium
 - “complex” bedrock geology, but alluvium is relatively homogeneous
- Goal: quantify scattering-generated shear waves
 - radial-to-transverse spectral ratios
 - wavefield mean-free-path (MFP)



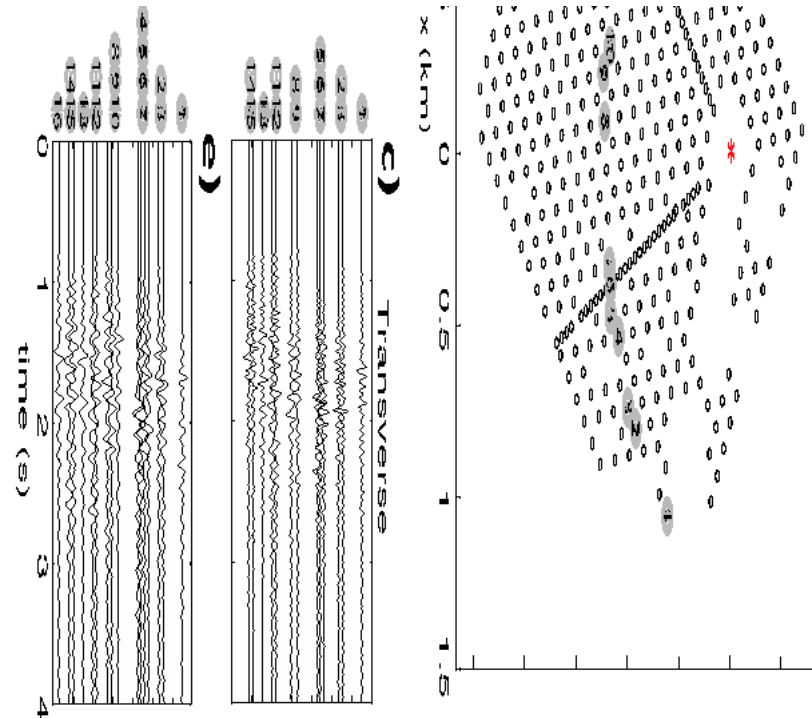
Darrh, A., Bodmer, M., Poppeliers, M., 2021. Spatially dependent seismic wavefield scattering from an underground chemical explosion: Analysis of the Source Physics Experiment Dry Alluvium Geology Large N array. **in review**

DAG: some raw data



DAG-3 →

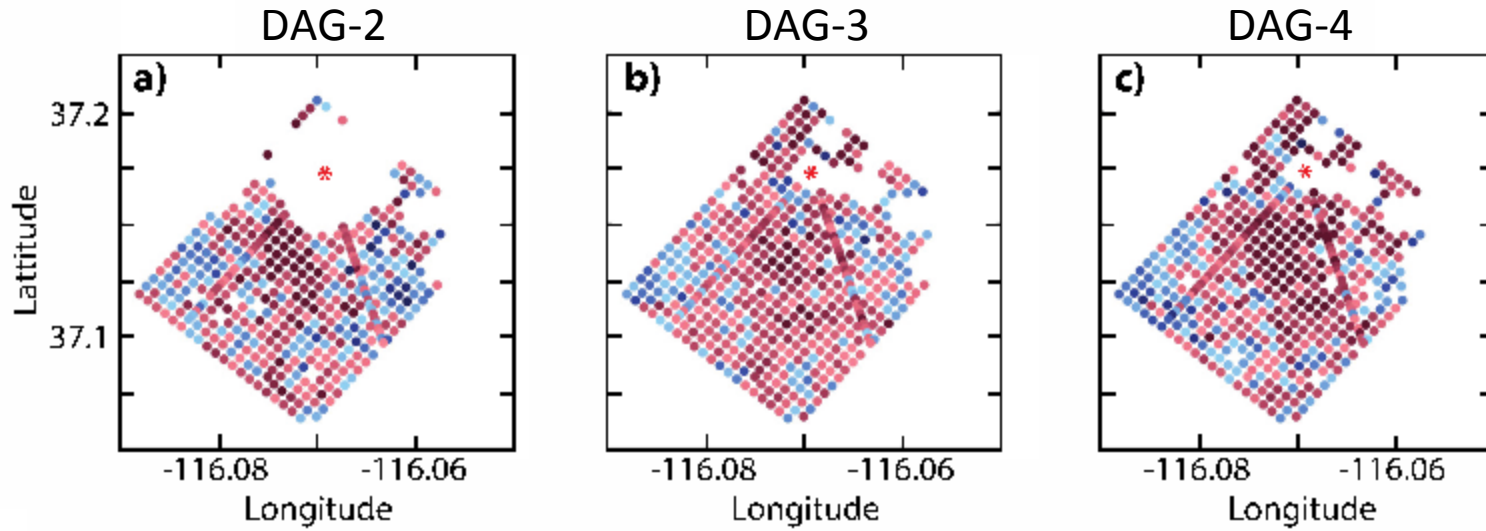
DAG-4 →



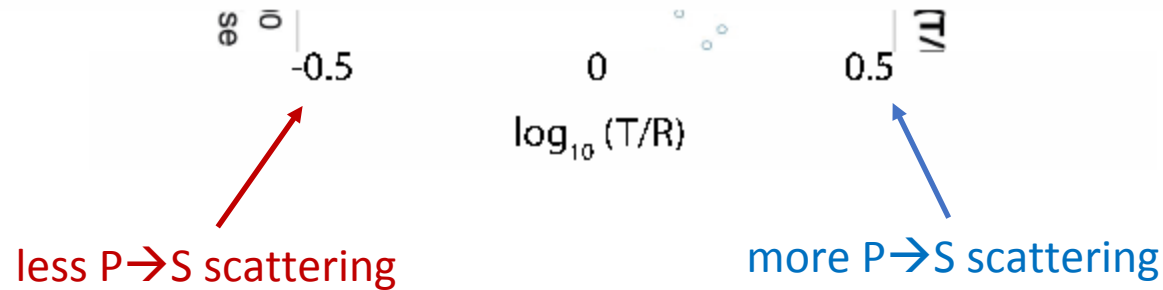
Preliminary observations show a marked radiation pattern

- 5-50 Hz passband
- all amplitudes trace normalized

DAG: transverse-to-radial energy ratio

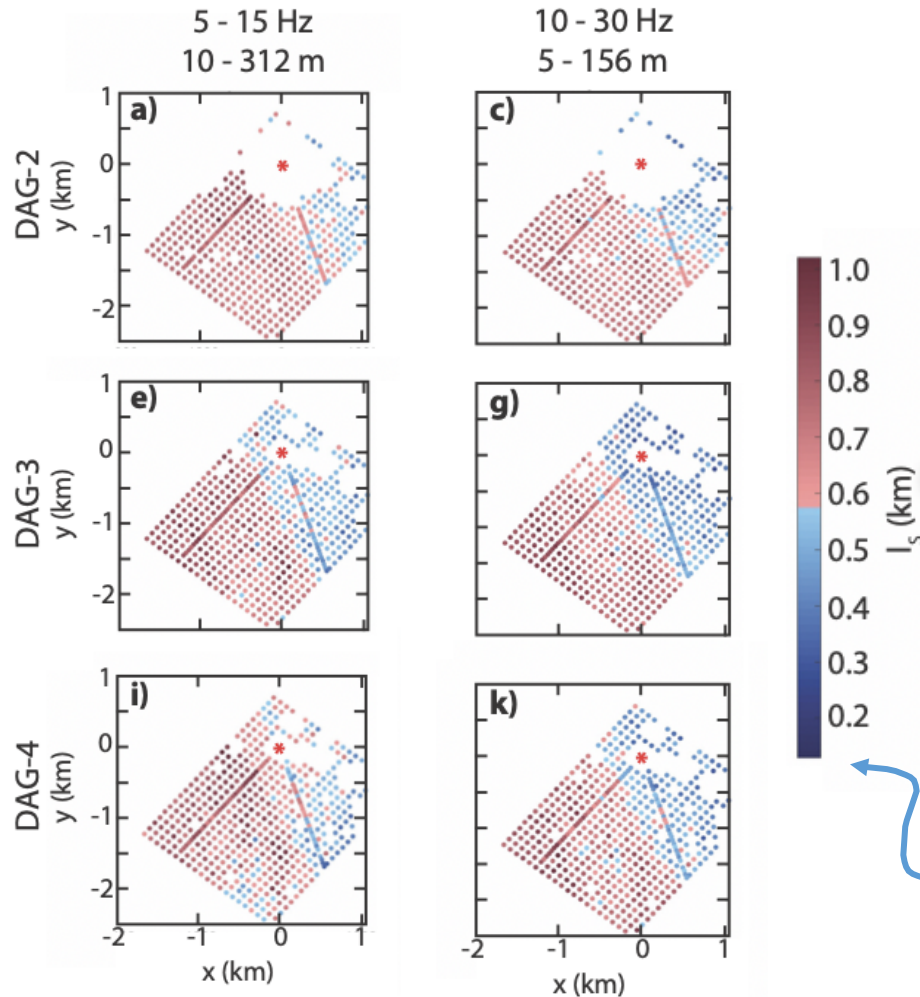


- Compare the root-mean-square energy ratio between the transverse- and radial-component seismograms, over the entire time-length, 5-50Hz*
- Results suggest less P-to-shear scattering to the south and more P-to-shear scattering to the west and east



$$* \frac{T}{R} = \frac{\sqrt{\frac{1}{N_t} \sum_t (u_k^{(T)}(x, y, t))^2}}{\sqrt{\frac{1}{N_t} \sum_t (u_k^{(R)}(x, y, t))^2}}$$

DAG: mean-free-path of scattered wavefield

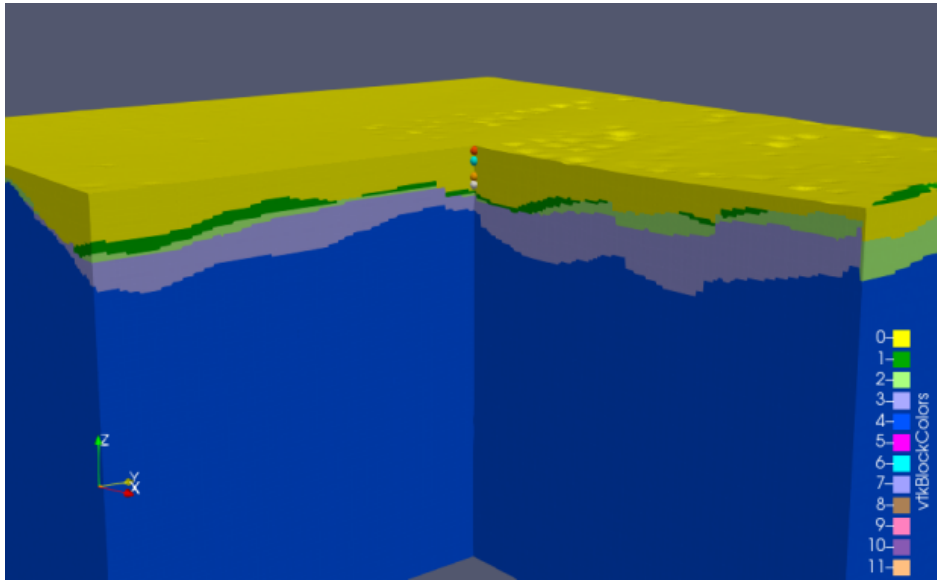


- Estimate mean-free-path (MFP) of scattered wavefield (mute direct P arrival)
- Analysis over two passbands
- Red indicates a longer MFP, or **less scattering**
- Blue indicates shorter MFP, or **more scattering**
- Results suggest less scattering to the south and more scattering to the east
 - Similar to T/R results!

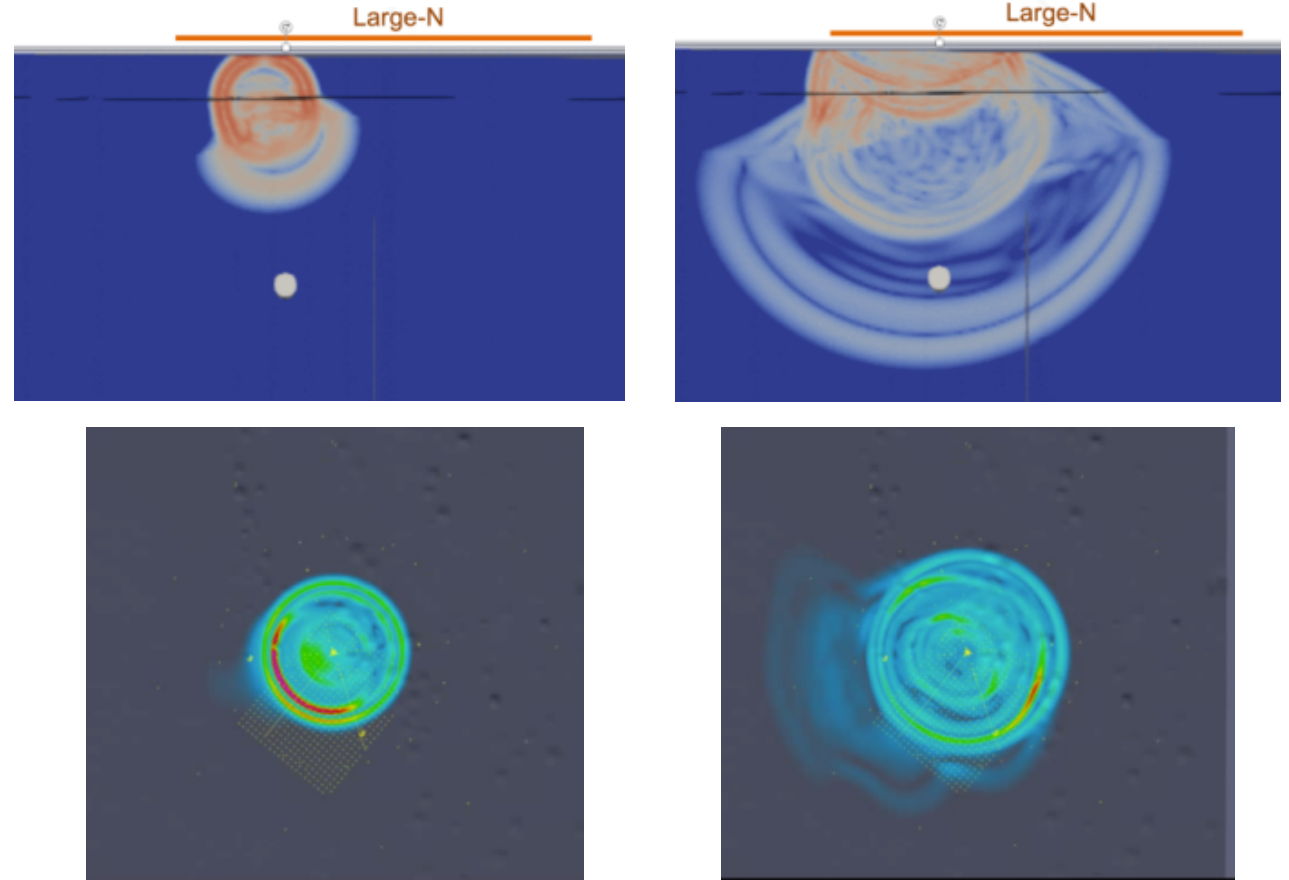
DAG: Modeling P-to-shear scattering: the effects of large-scale geologic structure



GFM model made-up of 5 geologic units.
(Prothro and Wagoner, 2020)

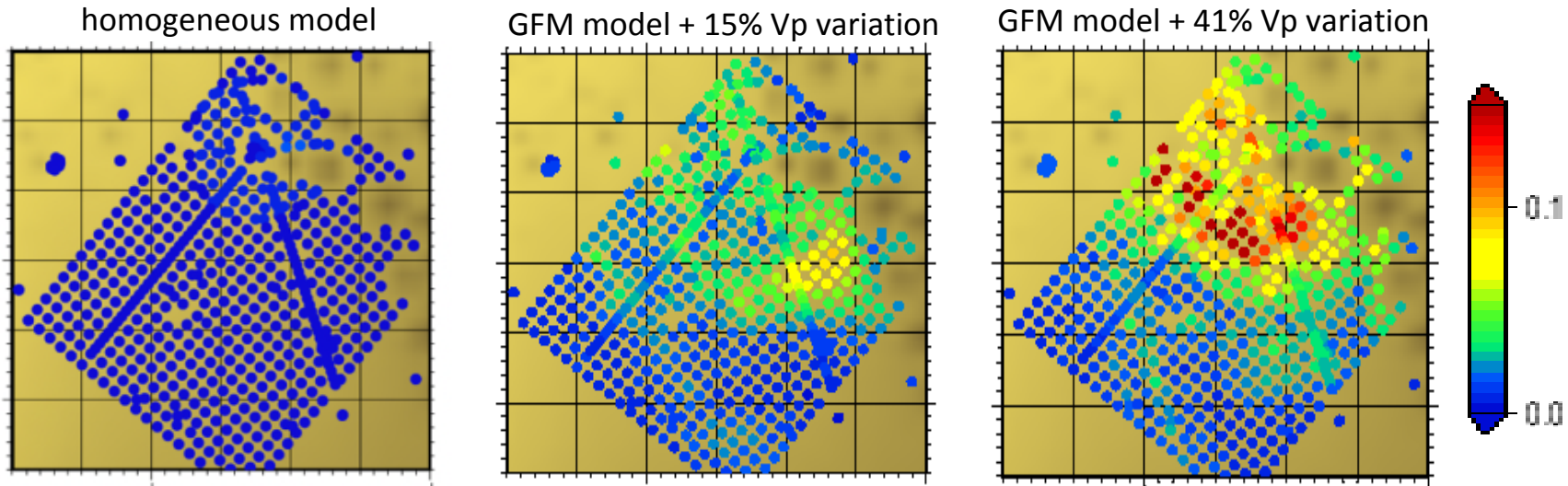


Modeling done with SPECFEM3D (spectral element)
with a mesh sustaining 25 Hz
MPI+GPU: 1272 cores in 30min for 7.5s seismograms
(images from Ting Chen and Carene Larmat, LANL)



Snapshots of transverse-component wavefield. Scattering produced by deterministic geologic structure in the GFM model.

DAG: Modeling P-to-shear scattering: the effects of large-scale geologic structure



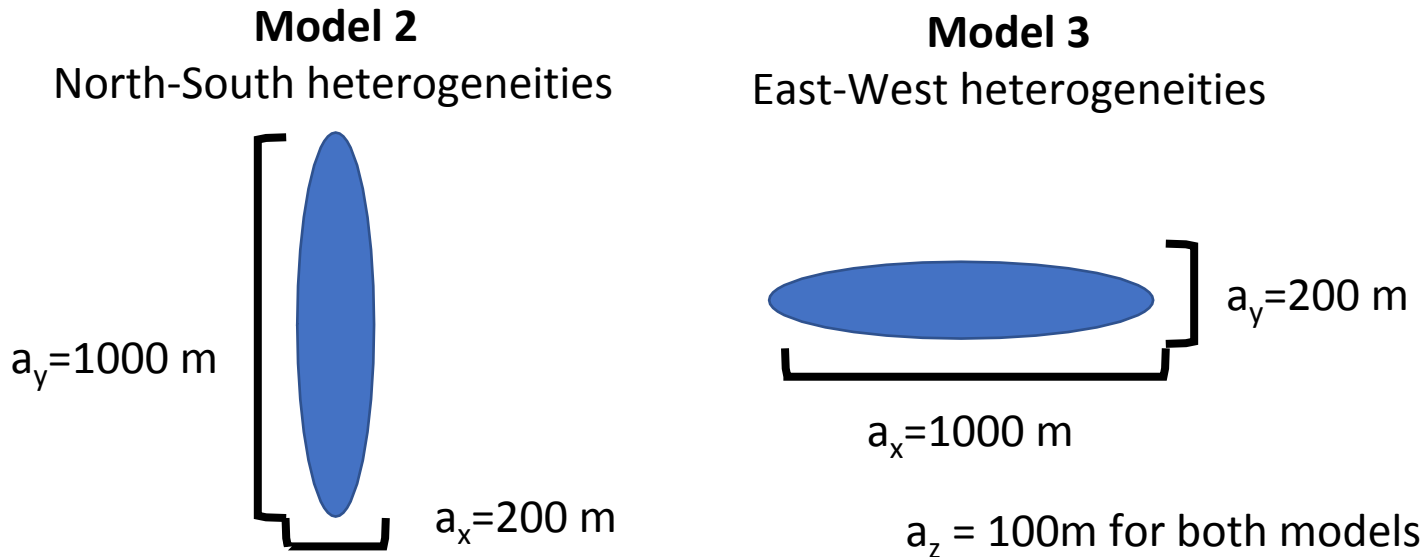
Peak velocity of low-pass (22Hz) transverse component of modeled waveform for the DAG GFM model but different elastic properties (images from Ting Chen and Carene Larmat, LANL)

- Simulations here show the effects of varying the degree of the seismic wavespeed for each geologic unit relative to the other units
- Each unit has a homogeneous wavespeed throughout
- Here, P-to-shear scattering is produced by P-to-shear conversions along the boundaries of the geologic units.
- Note that these results show more shear energy to the south and southeast suggesting that structure may be contributing to P-to-shear scattering

DAG: Modeling P-to-shear scattering: the effects of stochastic heterogeneity



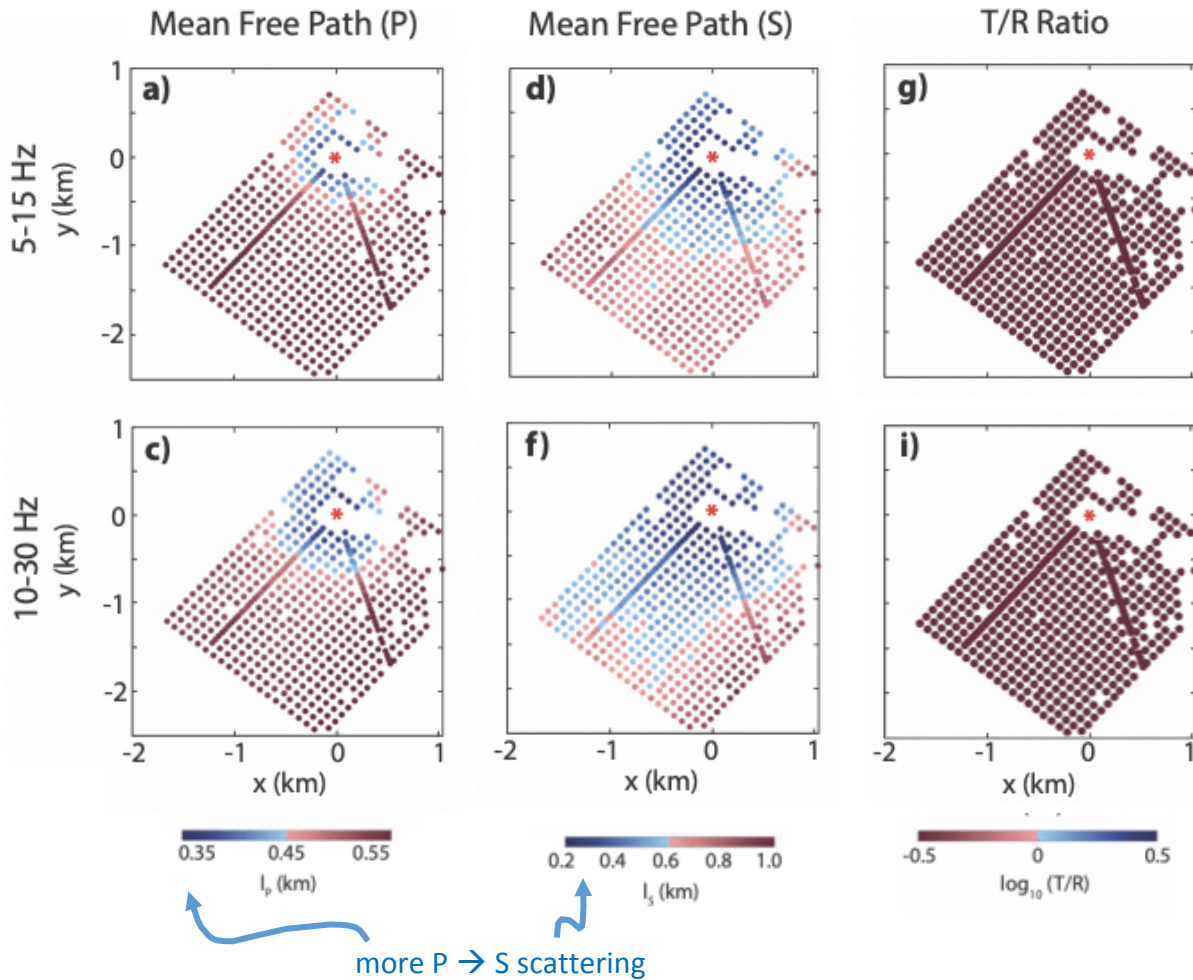
- Three synthetic tests* conducted:
 - Model 1: Geologic Framework Model (GFM) (Prothro & Wagoner, 2020) with no stochastic heterogeneities
 - Model 2: Halfspace model with stochastic heterogeneities** oriented North-South
 - Model 3: Halfspace model with stochastic heterogeneities oriented East-West



*3D elastic finite differences, 2m grid spacing, 30Hz maximum frequency, isotropic source at $z=100$ m

** von Karman stochastic model, with characteristic lengths defined by a_x , a_y , a_z , where the heterogeneities contain wavespeed/density contrasts of $\pm 14\%$ of the background

DAG: Modeling P-to-shear scattering: the effects of deterministic geologic structure



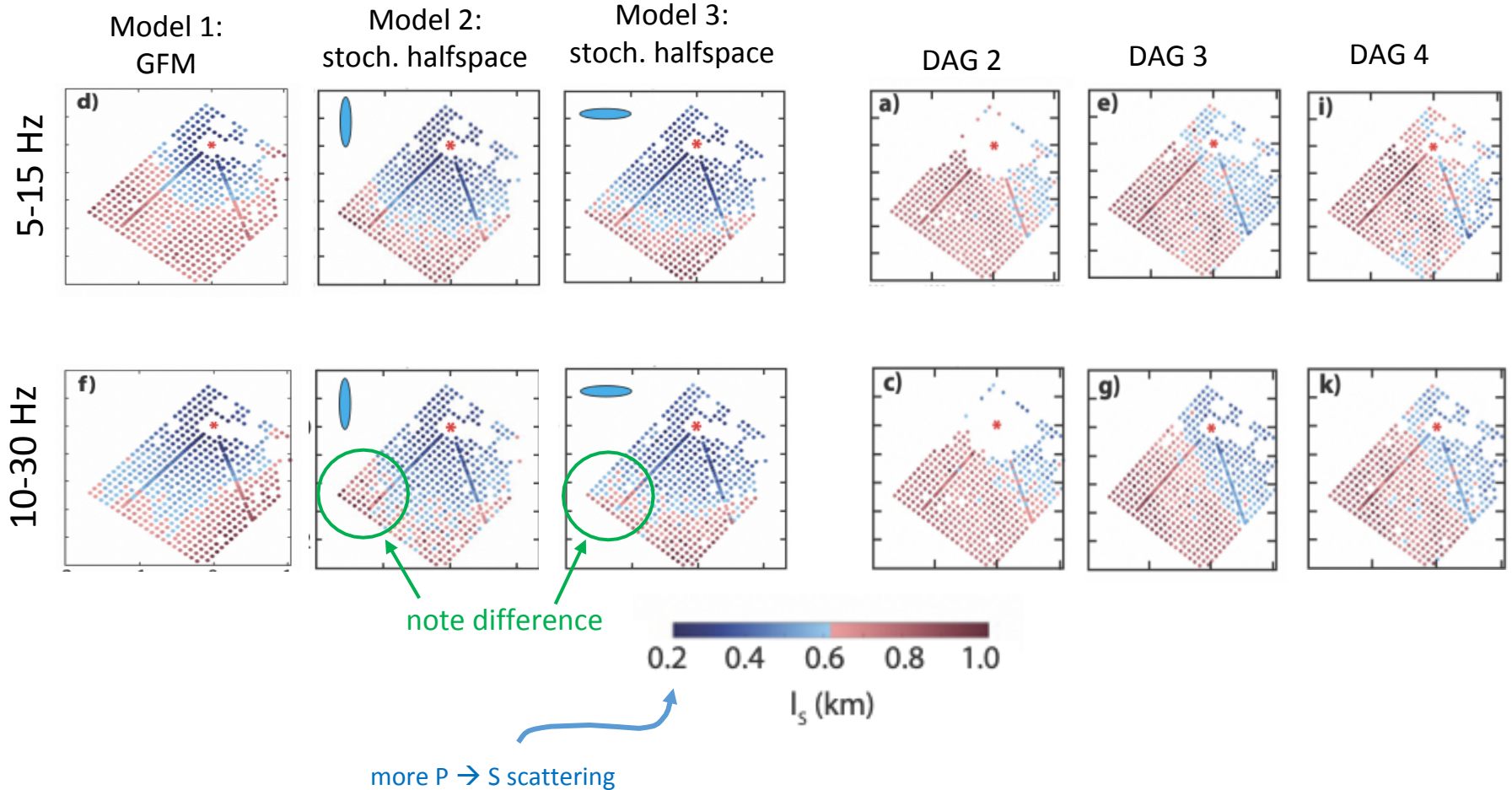
Model 1:

GFM with no stochastic heterogeneities
source depth = 100m

Simulation results/interpretations

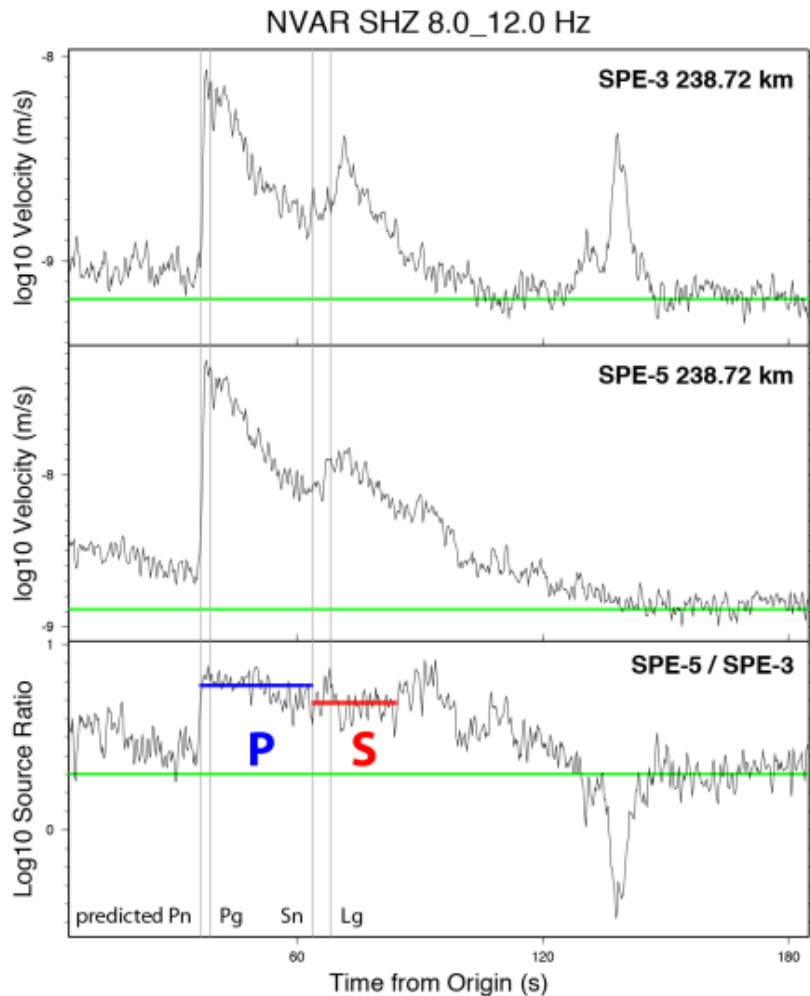
- MFP for P: No real azimuthal dependence for P-wave scattering over all passbands
- MFP for S: For 10-30Hz passband, there the MFP is shorter to the west and southwest, indicating more scattering in these direction.
- Because there are no stochastic heterogeneities in this model, the azimuthally-dependent MFP is due solely to large-scale geologic structure.
- T/R ratio is dominated by radially-polarized P waves.

DAG: Modeling P-to-shear scattering: the effects of stochastic heterogeneity: mean free path



- The GFM simulation does not reproduce the MFP obtained from the data, so bedrock structure is not likely the source of the anisotropic scattering
- Stochastic half-space simulations show that more scattering occurs in the direction of the long axis of the heterogeneities.
- NOTE: the stochastic halfspace models are not attempting to reproduce the data, rather show that preferentially aligned heterogeneities can influence the direction of scattering.

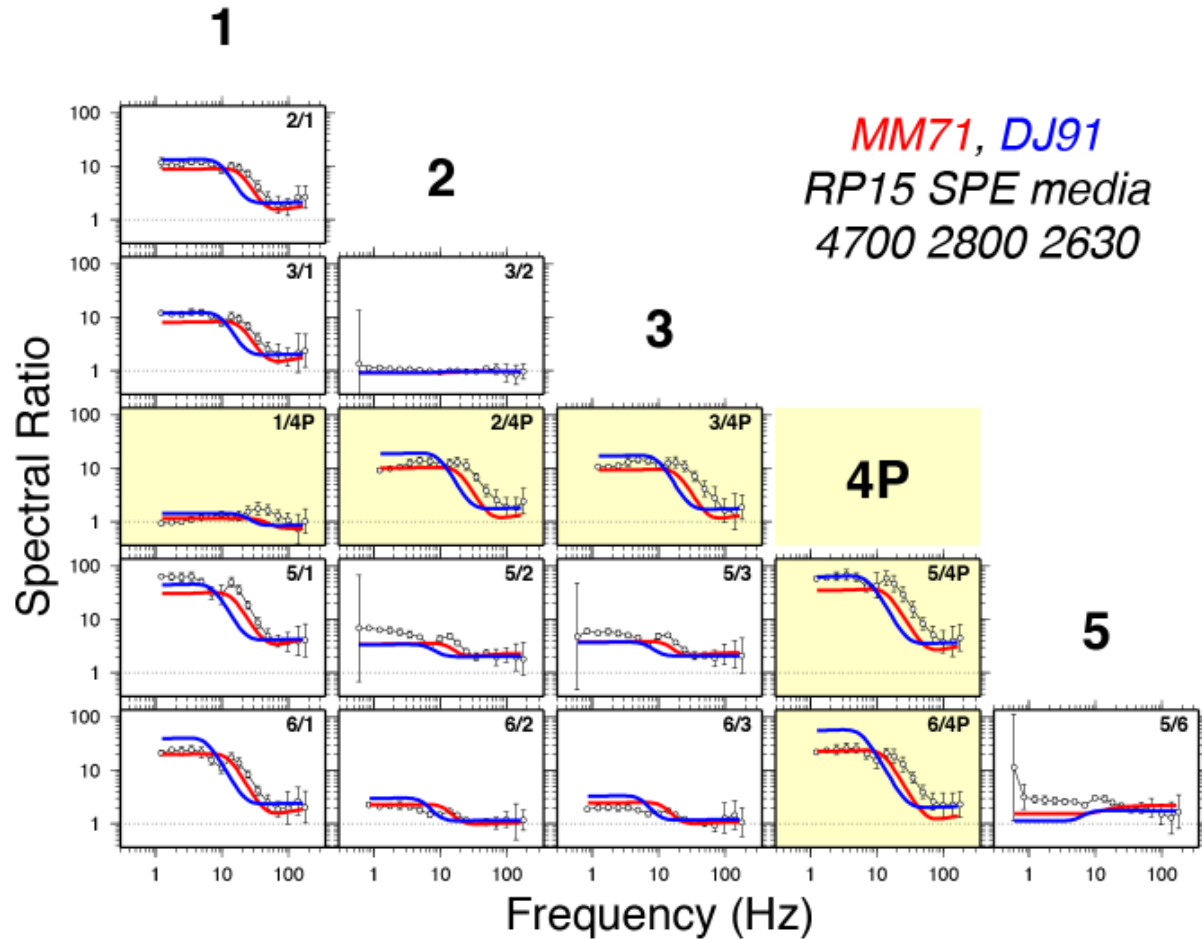
Shear generation from surface effects?



- Regional distance
- the ratio of enveloped seismograms suggest that the P and S ratios are different.
- SPE-5 and SPE-3 have different source depths, and hence differing amounts of surface interaction
- If NO surface interaction, then there would be no difference.
- Interpretation: surface effects (spall) generates Lg?

figures from Scott Phillips, LANL

Shear generation from surface effects?



- Regional distance
- SPE_i / SPE_j , but in the frequency domain
- Interpretation: surface effects (spall) generates L_g ?

figures from Scott Phillips, LANL

Conclusions



- Scattering from deterministic (geologic) structure has a strong influence on wave propagation direction and generates shear waves (P→S conversions)
- Scattering from stochastic heterogeneities generates a significant amount of seismic shear waves
- Shear wave generation from scattering is azimuthally anisotropic
- Scattering from heterogeneities appears to saturate at source-receiver distances greater than ~1km, depending on propagation azimuth and wavefield frequency

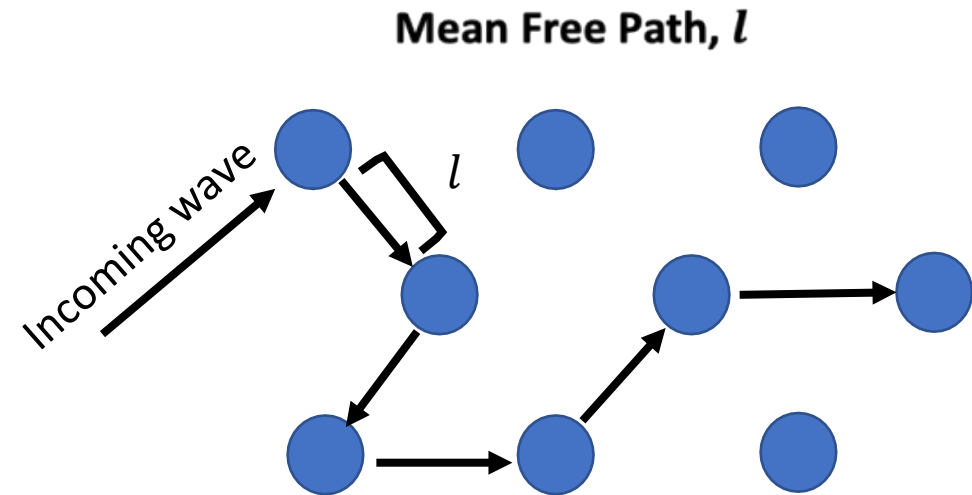
extra slides



SPE Phase 2 (DAG): Large N analysis strategy



- Transverse to radial energy ratio:
 - Isotropic explosive source in homogenous halfspace – no transverse component seismic wavefields should be generated
 - Used to identify areas with a high amount of transverse component energy
- Estimate mean free path:
 - Nonlinear inversion (deterministic)
 - Shorter mean free path indicates a higher amount of scattering
 - Used to estimate areas of spatially variable scattering



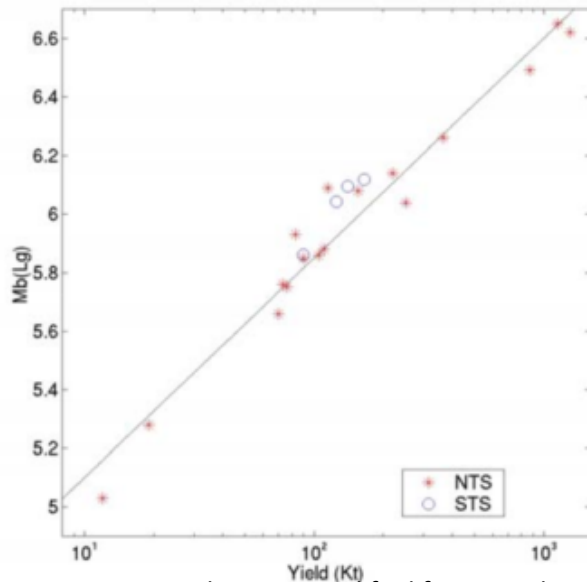
Goal of our Task: better understand/quantify/model seismic shear wave generation from buried explosions

- Why?

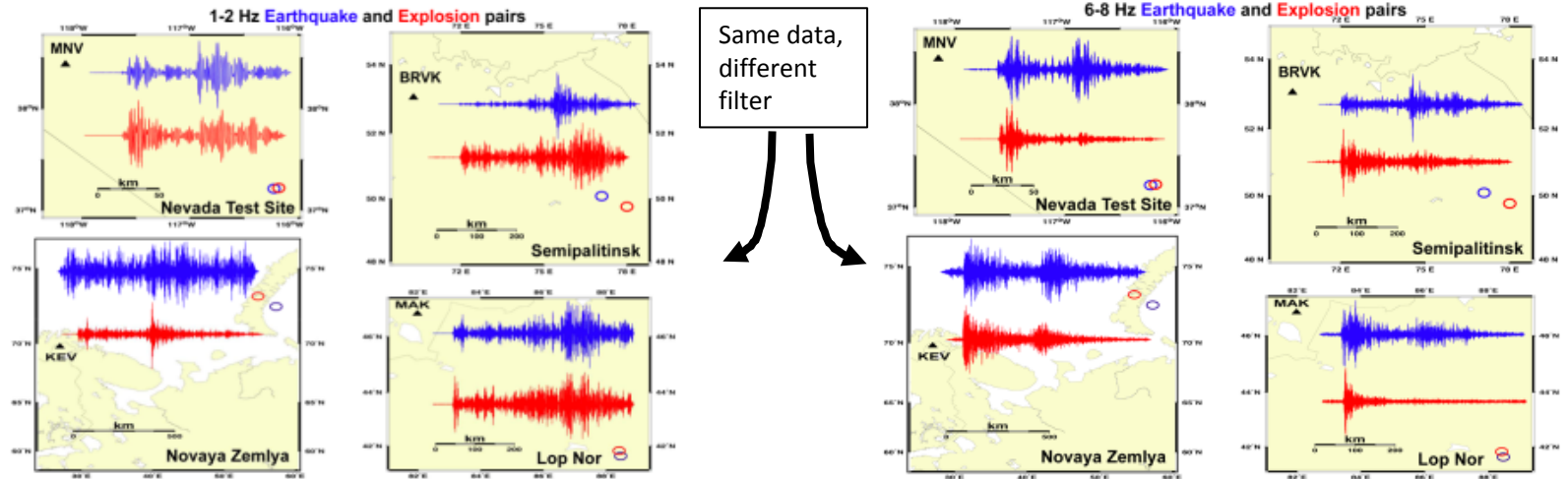
- “Global” observations: *sometimes* seismic shear waves are observed for buried explosion sources (in some cases).

“... 1-2 Hz seismograms of earthquake (red) and explosion (blue) pairs at nuclear test sites show little consistent relative P to S wave amplitude differences between the two source types. Low-Frequency P/S does not discriminate closely located events recorded on the same station at nuclear test sites.”

Lg amplitude vs. yield



(from Stevens et. al., 2004, modified from Nuttli, 1986a and Hansen et al., 1990))



From Walter et al., 2007, 29th Monitoring Research Review

Background



Explosion generated shear waves are likely generated via

1. surface spall → surface waves: Rg and Lg(?)
 1. “ground roll”
2. slip on pre-stressed fractures and faults → S body waves
 1. Expect that P/S ratio is NOT distant dependent
3. damage to hard-rock regions adjacent to the source
 1. Expect that P/S ratio is NOT distant dependent
4. P-to-shear conversions from scattering → surface and body waves
 1. Near source: expect that P/S ratio IS distant dependent
 2. “generalized”: expect that P/S ratio IS NOT distant dependent (scattering leads to saturation of shear waves)

SPE - I: wavefield coherency

Method:

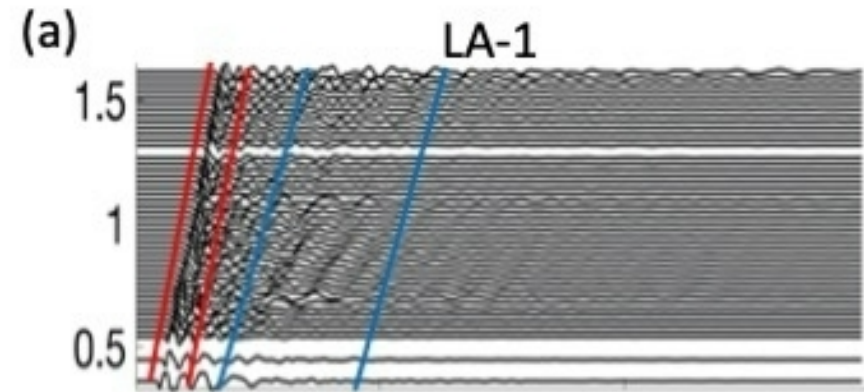
- quantify the coherency of the vertical-component seismic data as a function of frequency and propagation direction

$$MSC_{xy}(f) = \frac{|P_{xy}(f)|^2}{P_{xx}(f)P_{yy}(f)}$$

$P_{ij}(f)$ = the cross power spectral density for seismograms i and j .

$MSC_{xy}(f)$ is the “magnitude-squared coherency” between two time series, as a function of frequency. If $MSC_{xy} = 1$, then they’re perfectly similar

- Compute $MSC_{xy}(f)$ for each seismogram pair along each linear array for two time windows (P and “post-P”)



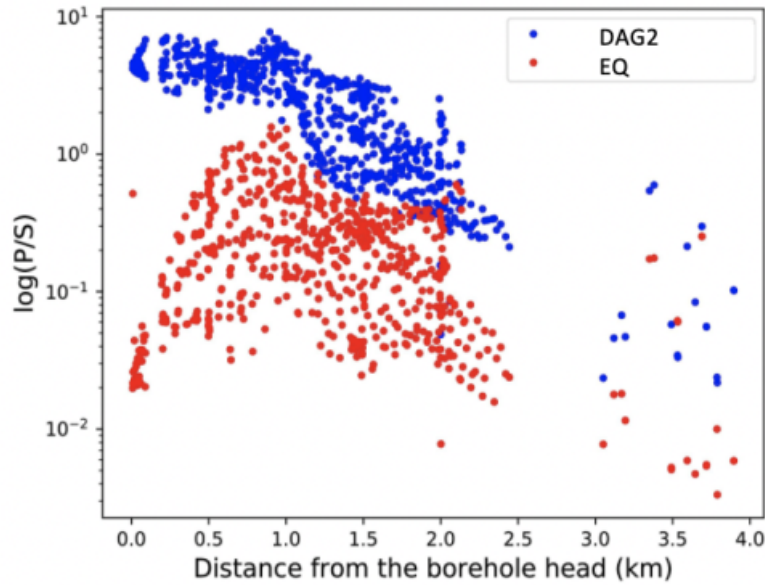
Extra slides from T. Chen and C. Larmat



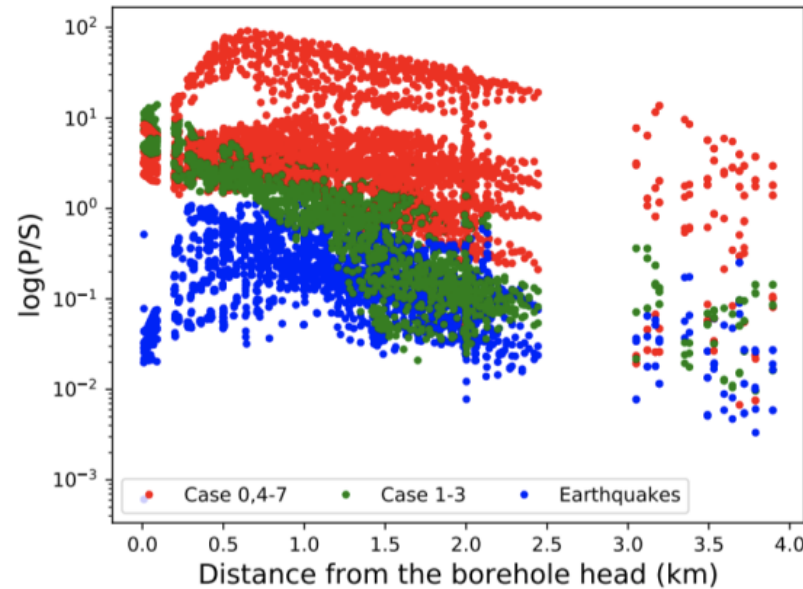
Testing the effect of 3D structure on P/S ratio discriminative power



Explosion vs. earthquake

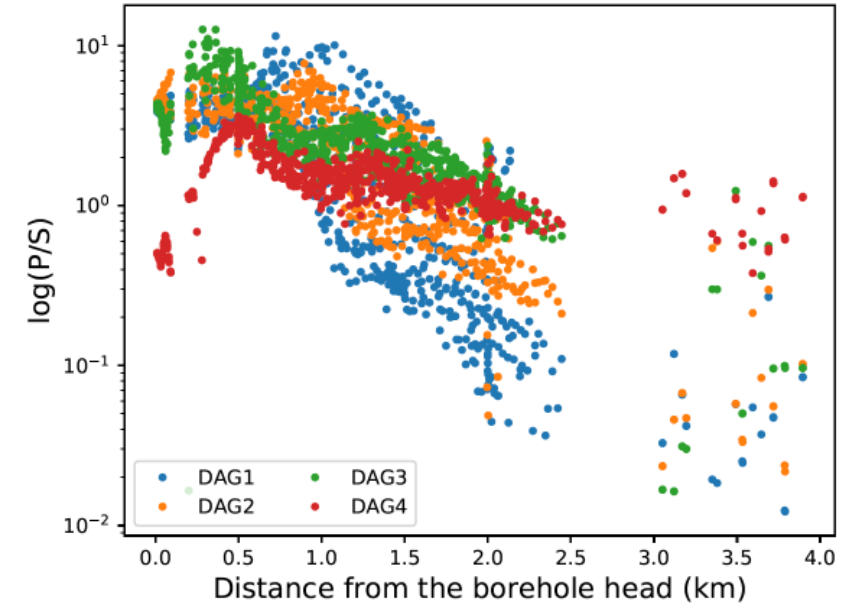


Different velocity models



case	Velocity Change of Medium (%)		
	Alluvium	Tuff	Paleozoic
0	0	0	0
1	-30	-30	+30
2	-30	+30	+30
3	-30	+30	-30
4	+30	+30	-30
5	+30	0	-30
6	+30	0	+30
7	homogeneous medium		

Different source depth



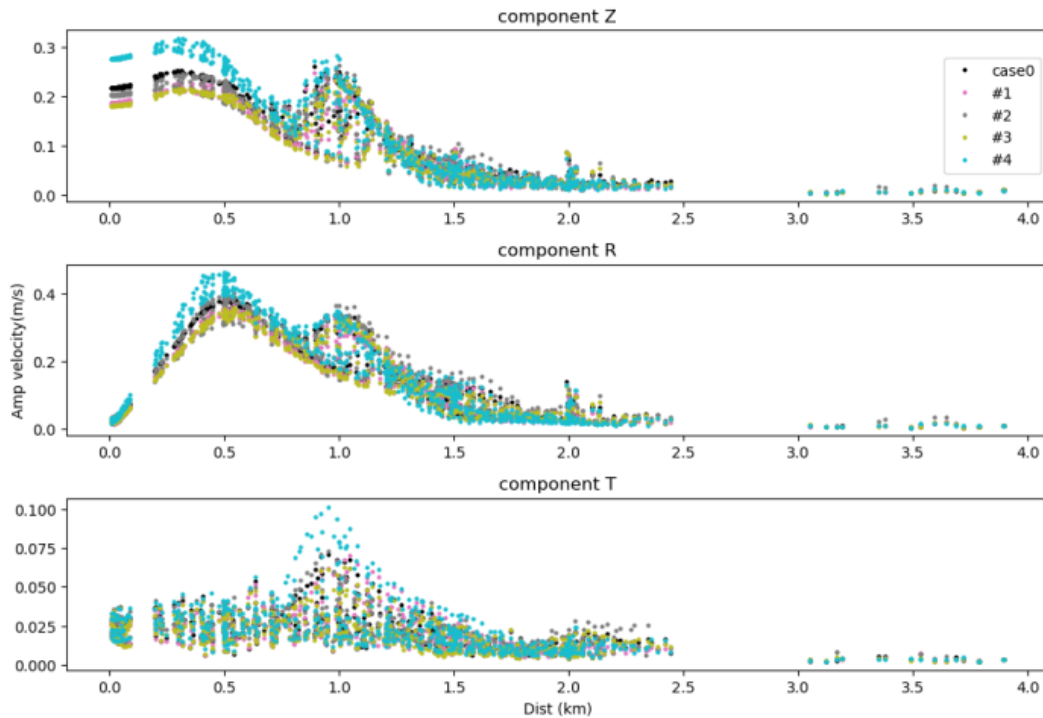
DAG-2	Explosion ($M_{rr}=M_{tt}=M_{pp}$)
EQ	Double-couple

DAG Explosion	Depth (m)
DAG-1	385
DAG-2	299.8
DAG-3	149.9
DAG-4	51.6

Generation of shear-wave by stochasticity

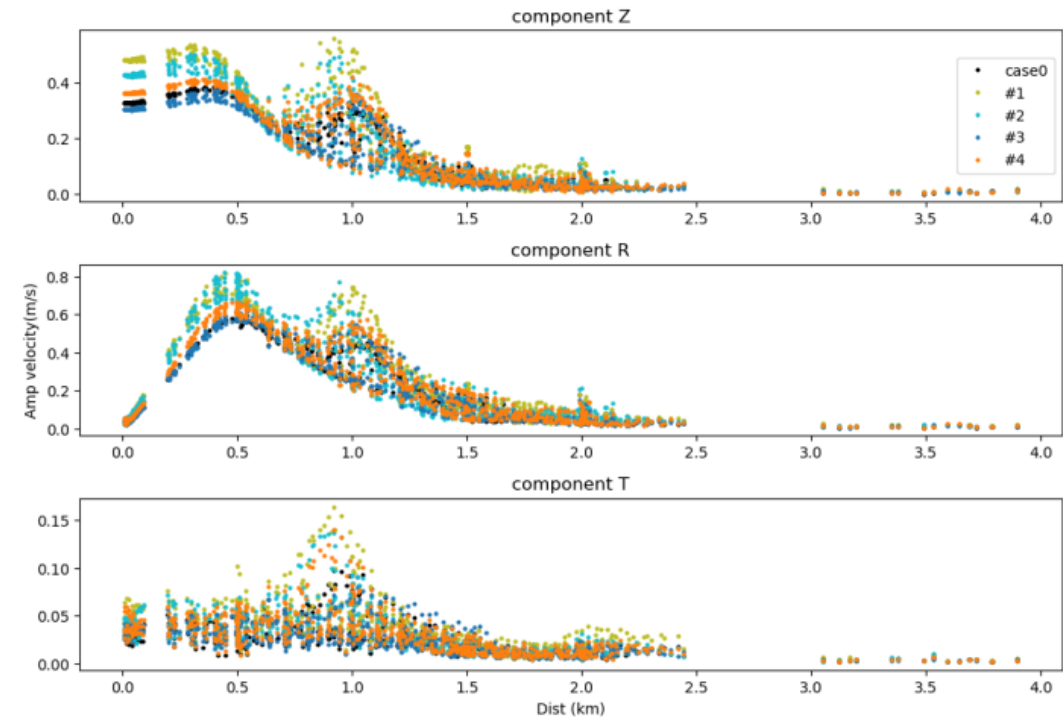


Comparison deterministic and heterogeneous model for DAG-2; low-pass 19Hz; 500m-30%



Peak velocity for the three components for stochastic variations of 30% and correlation lengths of 500m.

Comparison deterministic and heterogeneous data for DAG-2; low-pass 19Hz; 500-500-60m 30%



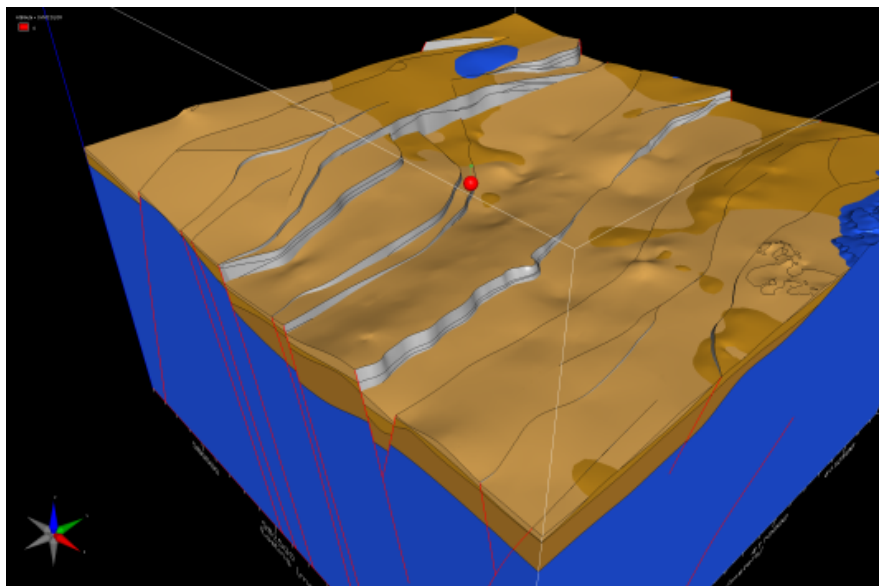
Peak velocity for the three components for stochastic variations of 30% and correlation lengths of 500m horizontally and 60m vertically.

Extra Slides from A. Pitarka



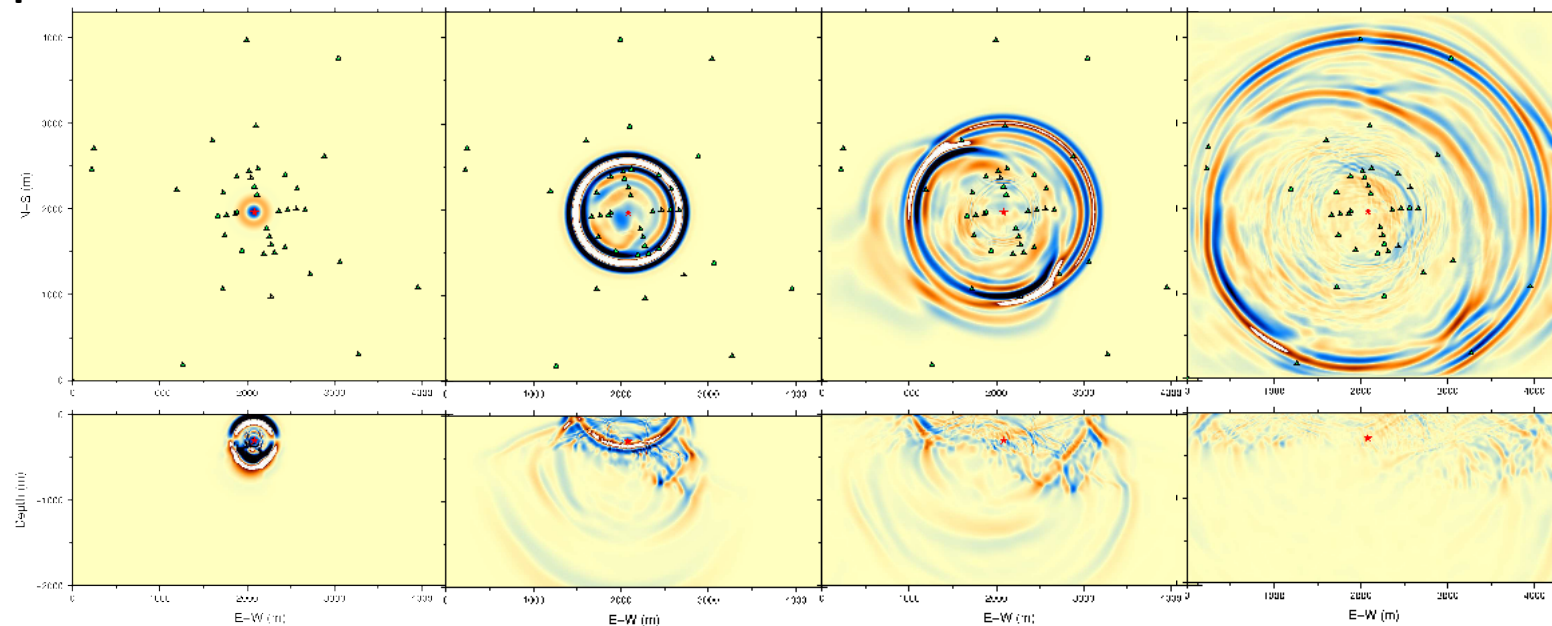
Underground Structure Complexities

1. Large-scale structural heterogeneity due to faulting
2. Source proximity to layers boundary with strong velocity contrast
3. Chimneys and craters from past nuclear shots.



Yucca Flat near U2ez
(alluvium removed)
Tertiary/Tuff
Paleozoic/Carbonate
basement

Wagoner et al.

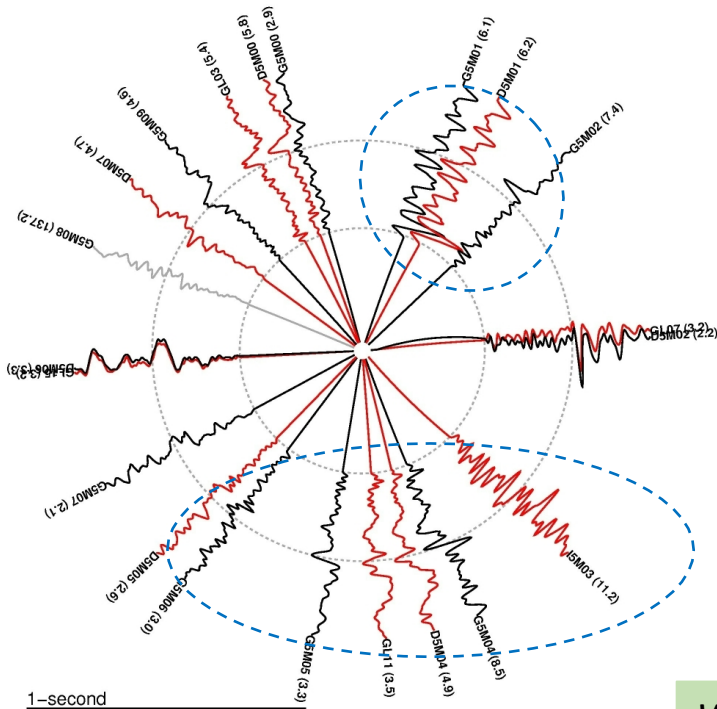
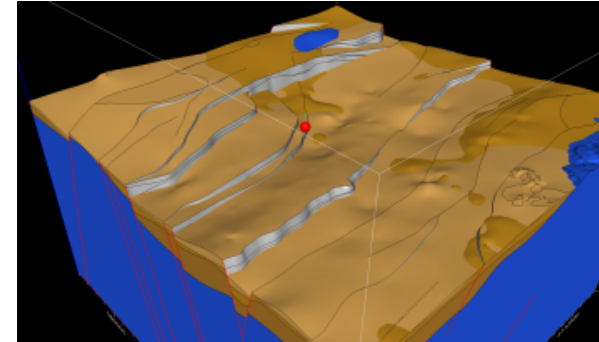


Snapshots of the Vertical Component of SIMULATED Ground Motion Velocity for DAG1

DAG-1

Transverse Displacement (microns)

black = geophones
red = broadbands



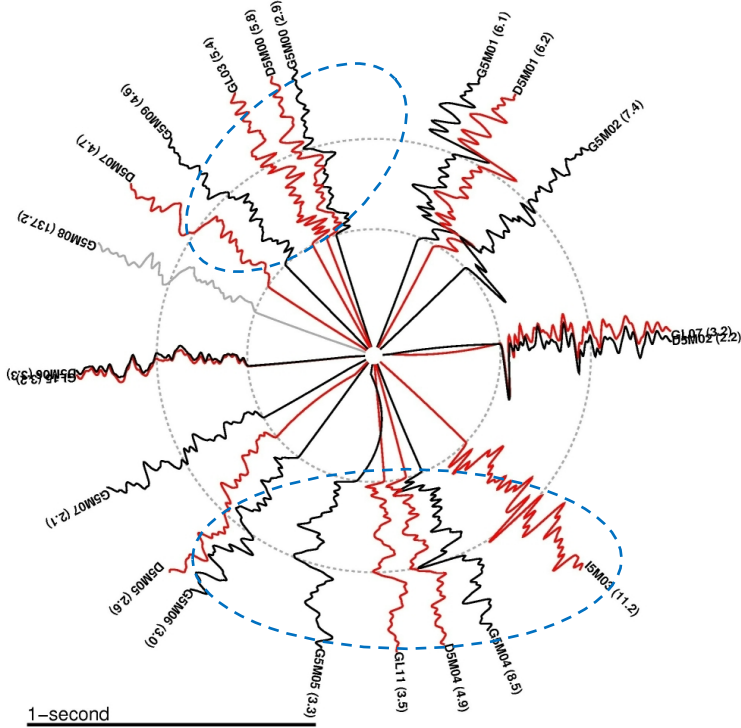
DAG-1 500m Ring **Transverse Components**

Wave train shear motion right after P wave

DAG-1

P/S
higher

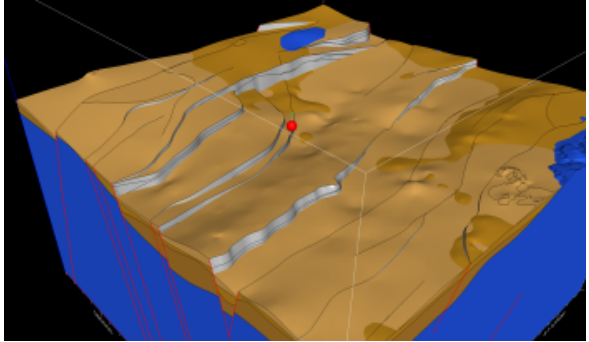
Radial Displacement (microns)



P/S lower
sharp S wave onset

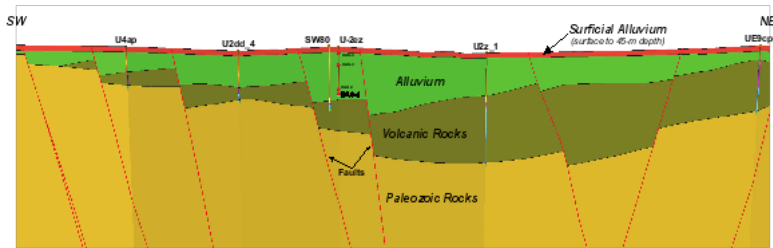
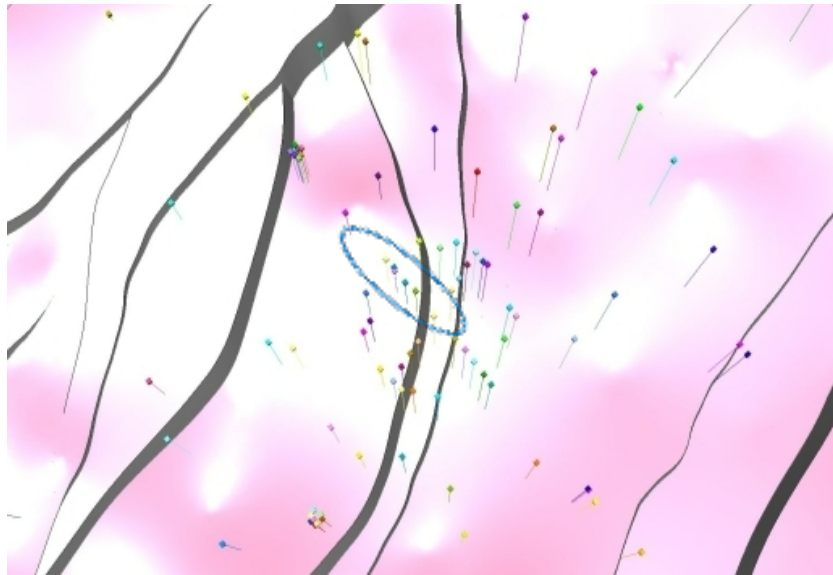
DAG-1 500m Ring Radial Components

black = geophones
red = broadbands

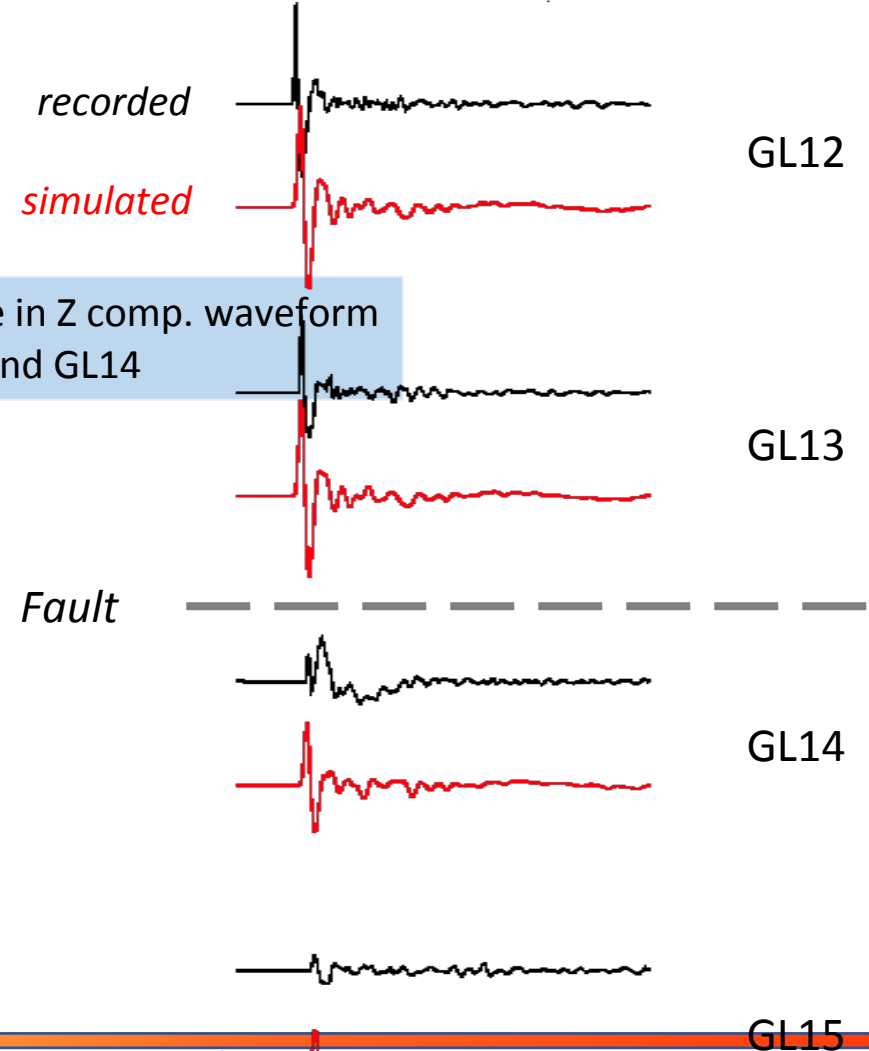


Fault scarp effect on recorded Z comp.

Paleozoic Surface (GFM)



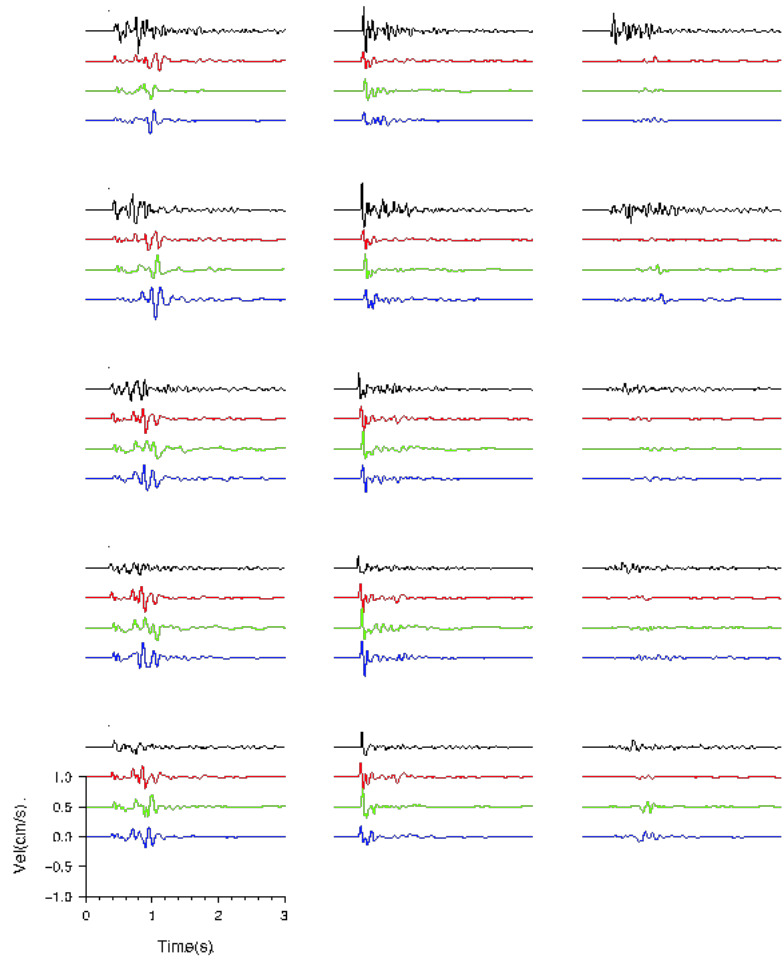
Note the change in Z comp. waveform between GL13 and GL14



Prothro, 2018

G5M 500m Ring Stations DAG-1 Simulation < 10Hz (soon 20Hz)

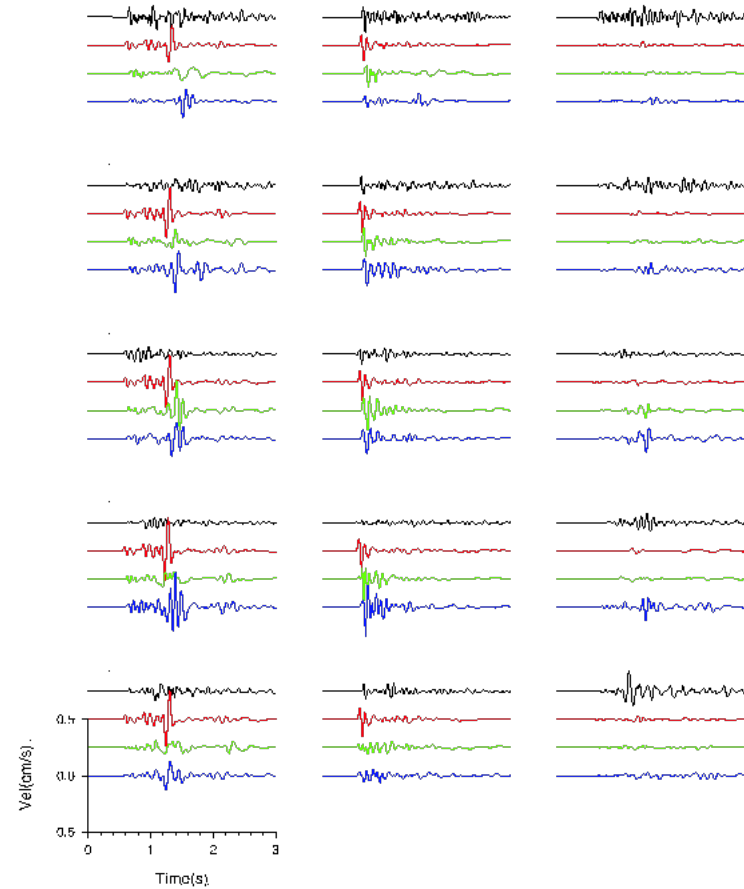
R=1500m



source contribution small

recorded
 1D * 2
 GFM * 2
 GFM-S * 2

R=500m



Double-pulse P wave from the source

Questions

